Analytical Structural Weight Estimation of Conceptual Launch Vehicle Fuselage Components with the Georgia Tech Structural Tool for Rapid Estimation of Shell Sizes (GT-STRESS)

Virgil L. Hutchinson, Jr.
Georgia Institute of Technology
AE 8900
Dr. John Olds, Advisor
May 3, 2004

Table of Contents

List of Figures

List of Tables

List of Symbols

%_fuel	percent fuel remaining
A	cross-sectional area
a	semi-major axis
A_f	stability frame cross-sectional area
axial_accel	axial acceleration
b	semi-minor axis
c	farthest from the neutral axis along the y-axis
C_f	Shanley constant (1/16,000)
cg	Center of Gravity
D	depth of cross section
d	component center of gravity location
E	Modulus of Elasticity
E_f	modulus of elasticity for the frame
$(EI)_f$	required stability frame stiffness
g_{axial}	axial acceleration
h	elliptical perimeter factor
h	liquid propellant height level
I	Area Moment of Inertia
I_y	Area Moment of Inertia with respect to y-axis
k_c	shape correction factor for circumference of non-circular shell cross sections
k_f	stability frame stiffness coefficient
K_{mg}	minimum gage parameter
L	stability frame spacing
lb	pound(s)
M	Bending Moment
m	minimum shell weight equation exponent
n	number of iterations
N_1	maximum principal stress
N_{eq}	equivalent running load in the material
norm_accel	normal acceleration

N_x	longitudinal running load
N_{xaxial}	axial force contribution to the longitudinal (axial) running load
N_{xbend}	bending stress contribution to the longitudinal (axial) running load
N_{xhead}	head pressure contribution to the longitudinal running load
$N_{xullage}$	ullage pressure contribution to the longitudinal running load
N_{xy}	transverse (shear) running load
N_y	circumferential running load
N_{yhead}	head pressure contribution to the circumferential running load
$N_{yullage}$	ullage pressure contribution to the circumferential running load
P	axial force
P_{ell}	perimeter of ellipse
p_{head}	head pressure
$P_{non\text{-}circular}$	perimeter of non-circular cross section
p_{ullage}	ullage pressure
r	radius
R^2	coefficient of variation
R_t	radius of curvature
t	total equivalent structure thickness
t_f	smeared equivalent stability frame thickness
t_{mg}	minimum gage thickness of material
t_s	equivalent shell thickness
$t_{s,B}$	equivalent shell thickness due to buckling failure
$t_{s,mg}$	equivalent shell thickness due to minimum gage restriction
$t_{s,UTS}$	equivalent shell thickness due to ultimate tensile strength failure
$t_{s,YS}$	equivalent shell thickness due to yield strength failure
V	shear force
W	component weight
W_{actual}	actual component weight
$W_{calculated}$	component weight from the current iteration
W'_f	stability frame weight per inch
W_{last}	component weight from the previous iteration

W_{next}	component weight value fed back to the weight definition
W_{PDCYL}	component weight calculated from PDCYL
W_{STRESS}	component weight calculated from GT-STRESS
W_T	total estimated structural weight
w_x	axial distributed load
w_y	normal distributed load
y	value of the estimated weight
α	convergence relaxation factor
β_0	y-intercept of the regression line
β_1	slope of the regression line
Δx	interval between each fuselage station
ε	shell buckling efficiency
θ_s	slope of beam deflection
ρ_c	Radius of Curvature in relation to the curvature of a beam
ρ_f	density of stability frame material
ρ_p	propellant density
ρ_s	density of shell material
σ_{axial}	axial stress
σ_{bend}	bending stress
σ_{eq}	equivalent stress in the material
σ_h	normal stress in hoop (circumferential) direction
σ_{hhead}	normal stress due to head pressure in hoop (circumferential) direction
$\sigma_{hullage}$	normal stress due to ullage pressure in hoop (circumferential) direction
σ_l	normal stress in axial (longitudinal) direction
σ_{lhead}	normal stress due to head pressure in axial (longitudinal) direction
$\sigma_{lullage}$	normal stress due to ullage pressure in axial (longitudinal) direction
$\sigma_{maxbend}$	maximum bending stress
σ_{UTS}	ultimate tensile strength
σ_{YS}	yield strength
τ_{max}	maximum shear stress
τ_{xymax}	maximum shear stress

Abstract

Many conceptual launch vehicles are designed by the integration of various disciplines, such as aerodynamics, propulsion, trajectory, weights, and aeroheating. In the determination of the total vehicle weight, a large percentage of the vehicle weight is composed of the structural weight of the vehicle subsystems, such as propellant tanks. The weight of each subsystem is derived from the material composition and structural configuration required to withstand the load conditions it experiences during the vehicle operation.

Mass estimating relations (MERs) are often used to estimate the vehicle structural weight in relation to geometric parameters of the vehicle. MERs created from data available from existing vehicles are only valid for the load conditions experienced by those particular vehicles and they may not take into account the variation in load conditions due to a vehicle's trajectory or weight. The vehicle structural weight can also be determined using multi-dimensional finite element (FE) models. Though this high-fidelity technique provides very accurate results, the creation, preparation, and analysis of complex FE models to predict structural weight can require a large amount of computational effort and can also be very time consuming.

Instead of employing multi-dimensional FE models, a simplified beam approximation model of the vehicle can be used for structural weight estimation. The vehicle is modeled as a simply supported beam defined by a sequence of cross sections. The inert masses, propellant masses, and accelerations are modeled as point and distributed loads over their position in the fuselage. The running loads required to size the thickness of the surface panels are calculated using a simply supported beam theory with the distributed loads on the beam as a function of axial and circumferential position. From the determined panel thickness and material properties, the structural weight is calculated. Estimating the tank structural weight requires minimum computational effort and time while providing accurate results. This study discusses the beam structural analytical method, describes the implementation of the technique into a software tool based upon the RL computer program to calculate running loads[4], and explores the application of the simplified beam approximation method to the weight estimation for structural components of an Evolved Expendable Launch Vehicle (EELV) and the External Tank of the Space Shuttle.

Introduction

Conceptual launch vehicle design involves the integration of various disciplines to generate a complete vehicle design. Disciplines included in the conceptual design synthesis are aerodynamics, propulsion, trajectory, weight and sizing, and aeroheating. The estimated vehicle weight is an important parameter involved in acquiring the required information from each discipline. Aerodynamic coefficients, required thrust, projected trajectory, and sized propellant masses are all direct and indirect functions of the vehicle weight. In the determination of the total vehicle weight, a large percentage of the vehicle weight is composed of the structural weight of the vehicle subsystems, such as propellant tanks, interstages, and fuselage structure. The weight of each subsystem is derived from the material composition and structural configuration required to withstand the load conditions it experiences during the vehicle operation.

There are two methods commonly used by the aerospace industry to estimate the load-bearing structural weight of launch vehicles: empirical mass estimating relations (MERs) determined from existing vehicle data and detailed finite element structural analysis. Empirical regressions of existing vehicle structure data that form the MERs to calculate structural weight are not capable of considering the varying load conditions that a particular vehicle experiences due to its trajectory or weight. The creation, preparation, and analysis of complex multi-dimensional finite element models provide an accurate prediction of the load-bearing structural weight, but this procedure can require a large amount of computational effort and can also be very time consuming.

Instead of employing these traditionally defined techniques, a methodology based on fundamental beam structural analysis has been developed for the rapid estimation of the load-bearing structural weight of the launch vehicle fuselage and its associated components. By creating a simplified beam approximation model of the vehicle, the method utilizes the vehicle component weights, load conditions, and basic material properties to analytically estimate the structural shell and stability frame weight. Implementation of this methodology into a fast-acting software tool for conceptual design resulted in the creation of a computer program, Georgia Tech Structural Tool for Rapid Estimation of Shell Sizes (GT-STRESS). The input format and basic operation of GT-STRESS is derived from RL, a computer program to calculate fuselage running loads, which was developed by Jeff Cerro, formerly of Lockheed Martin Engineering & Science

Services. The method was applied to an existing Evolved Expendable Launch Vehicle (EELV) and the External Tank (ET) of the Space Shuttle for verification and correlation. Using statistical techniques, the relationship between the estimated load-bearing structure weight calculated by GT-STRESS and the actual structure weights were determined.

Motivation

Current Methods of Weight Estimation

Two methods commonly available to the aerospace industry for the estimation of load-bearing structural weight for launch vehicle fuselage and its associated components are empirical mass estimating relations (MERs) and detailed finite element structural analysis. The advantages and limitations of each method presents are expounded within the following sections.

Mass Estimating Relations

Empirical MERs are the least complex method for weight estimation. Information of fuselage component weights from a database of existing vehicles in addition to various key configuration parameters of the vehicle are required to produce a linear regression of the data. The regression results in an equation for the component structural weight as a function of the configuration parameter for the existing vehicle. The configuration parameter is then scaled to determine an estimate of the component structural weight for the vehicle under investigation.
Accuracy of the weight predicted from MERs depends upon the quality and quantity of the database available for existing vehicles and the similarity of the weight and configuration between the vehicle under investigation and the existing launch vehicles. Though empirical MERs are lower fidelity methods for weight estimation, the rapid weight approximation from the regression equations allow them to be very useful in conceptual design.

Finite Element Analysis

Finite element analysis (FEA) is described as *the matrix method of solution of a discretized model of a structure*.[1] Structures are modeled as a multi-dimensional system of discrete (or finite) elements connected together at nodal points. Each element possesses a certain geometric composition and set of physical characteristics. Forces are applied at nodal points, and each point is capable of displacement. Mathematical equations are formed for each element relating the displacements of its surrounding nodal points to the corresponding nodal forces.[1]

The assembly of elements representing the entire structure is a large set of simultaneous equations that, when combined with the loading condition and physical constraints on the structure, are solved to find the unknown nodal forces and displacements. The resulting nodal forces and displacements are then replaced into each element to generate stress and strain distributions for the entire structural model. The stress and strain distributions are then exported to a structural sizing program to determine the unit weight of the elements over the entire structural model.[1]

Improved, Intermediate Method Needed

Preliminary subsystem weights of conceptual launch vehicles are conventionally obtained from MERs based on the regression of existing vehicles. This method is not always preferred and reliable for studies of unconventional vehicle concepts. Since the weight estimations are based upon existing vehicles, their application to unconventional configurations and loading conditions are questionable. For instance, the use of aircraft MERs to determine the structural weight of a horizontal take-off and landing reusable launch vehicle may be suspect due to the fact that the configuration and loading conditions of the vehicle with an orbital trajectory will be vastly different than that of a conventional aircraft. Also, these relations do not provide a straightforward method to assess the impact of advanced technologies and materials to the vehicle weight.

Finite element structural analysis methods for determining structural weight are often inappropriate for conceptual design. The idealized structural model of the vehicle must be created off-line and is incapable to being subjected to dynamic changes due to modifications in other vehicle parameters. The analysis of a moderately complex finite-element models can require a large amount of computational effort and can also be very time consuming, which can lead to a bottleneck in the vehicle design synthesis. For these reasons, the finite-element method is more relevant for use in detailed vehicle design.

In order to develop a method to accurately determine structural weight of the vehicle fuselage and components at a minimized cost of time and computational effort, an analytical approach that uses beam theory structural analysis was formed. A simplified beam approximation model of the vehicle is created for structural weight estimation. The vehicle is modeled as a simply supported beam defined by a sequence of cross sections. The inert masses, propellant masses, and accelerations are modeled as point and distributed loads over their position along the longitudinal axis of the fuselage. The running loads required to size the thickness of the fuselage and component shells are calculated using a simply supported beam theory with the distributed loads on the beam as a function of axial and circumferential position. From the determined panel thickness and material properties, the structural weight is calculated. Since the analysis is conducted station-by-station along the fuselage, the distribution of the loads and vehicle geometry are accounted for, which gives an integrated weight that accounts for local conditions.

The approach of an analysis based exclusively on fundamental structural principals will result in an accurate estimation of the vehicle structural weight only. Non-optimum weights for fuselage and component primary structure, such as bulkheads, minor frames, coverings, fasteners, and joints, are not estimated within the structural analysis and must be predicted from correlation to existing vehicles.

Overview of Procedure

Prior to the start of the actual analysis, the vehicle geometry and preliminary subsystem weights are defined along the fuselage. The vehicle geometry is modeled by a sequence of elliptical cross sections, which are defined by their location, semi-major axis, and semi-minor axis. The locations and weights of the inert masses and propellant masses are also defined, along with the accelerations, percentage of propellant available, and ullage pressure for each load condition. Detailed structural analysis of the fuselage begins with the calculation of the vehicle center of gravity, which allows for the determination of the simple support reaction loads. The combination of the defined vehicle weights and reaction loads are used for the integral calculation of vehicle loads on a station-by-station basis. The three types of external loads considered are axial force, shear force, and bending moment. These three stress resultants are calculated for each defined load condition at each fuselage station. The calculations of all the stress resultants consider the acceleration and amount of propellant available for each load condition.

After determining the external loads along each station of the fuselage, the in-plane shell stress resultants or running loads are calculated. The longitudinal bending moment, longitudinal axial, and transverse (shear) running loads are functions of their associated external loads and the cross section parameters. Contributions from the internal pressure running loads in the propellant tank area of the fuselage to the longitudinal and circumferential running loads are computed based on the ullage pressure and head pressure for each load condition. Once the running loads are determined at each fuselage station for each load condition, the maximum running load from the entire set of defined load conditions are selected to be used to determine the amount of shell material required at each section based on a *worst-case scenario*.

The maximum running loads at each fuselage station are used to calculate the amount of material required to preclude failure at the most critical point. The most critical point of the cross section is assumed to be the outermost location of the shell circumference. The failure modes considered are ultimate strength, yield strength, and buckling. A material minimum gage restriction is also imposed as a final failure criterion. There are also three types of stiffened shell configurations available for prevention of buckling failure of the fuselage shell structure: simple integrally stiffened shell concept, Z-stiffened shells, and a truss-core sandwich shell design.[2] Each shell configuration is accompanied with longitudinal frames to prevent general instability.

The material properties for the fuselage and its associated components are assumed isotropic and homogeneous, which include a generic laminate and core configuration of a composite material. From utilizing the failure criterion and selecting the appropriate shell configuration and material, the shell and frame thickness at each fuselage station are determined. The calculated shell and frame thickness are integrated station-by-station to ascertain the structural weight of the vehicle fuselage and components.

Vehicle Geometry

The geometry of the vehicle fuselage is modeled as a sequence of elliptical cross-sections centered about the longitudinal axis. Each cross-section is defined by its position along the longitudinal axis of the fuselage, semi-major axis, and semi-minor axis. The semi-major and semi-minor axes of cross-sections at undefined fuselage stations are determined from linear interpolation between the two defined boundary cross-sections. A visual representation of the geometric approximation of the vehicle is presented in Figure 1.

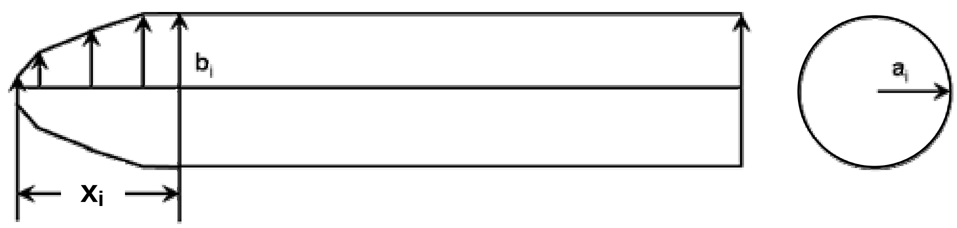

Figure 1. Visual Representation of Vehicle Geometry Approximation.

The use of elliptical cross-sections allows for the modeling of conceptual vehicles with a circular cross-section fuselage, slightly elliptical fuselage, or varying cross-sections shape along the fuselage length. The beam theory structural analysis utilized by this analytical method to determine the external stress resultants on the fuselage does not require any cross-sectional information. Yet in order to calculate the longitudinal axial and transverse internal running loads from the external stress resultants, the cross-sectional area at each fuselage station is required. The cross-sectional area of the shell is calculated from the product of the shell thickness and the cross-section perimeter. The perimeter of the elliptical cross section is ascertained using the S. Ramanujan approximation formula[3]:

$$P_{ell} = \pi(a+b)\left(1+\frac{3h}{10+\sqrt{4-3h}}\right), \text{ where } h=\frac{(a-b)^2}{(a+b)^2} \tag{1}$$

The maximum error of this formula for determining the elliptical perimeter is -0.04%.[3]

Weights Definition

After defining the geometry, the vehicle inert and propellant masses are mapped onto the beam approximation model of the vehicle. Inert masses and propellant masses are modeled as point and distributed loads over their position along the longitudinal axis of the fuselage in both the normal and axial directions. The weights are defined by the starting and ending position of the loading, and the total weight to be distributed over the range of the load. For weights acting at a single point on the vehicle, the starting and ending position of the load are the same. A visual representation of the masses mapped onto the beam approximation of the vehicle is presented in Figure 2.

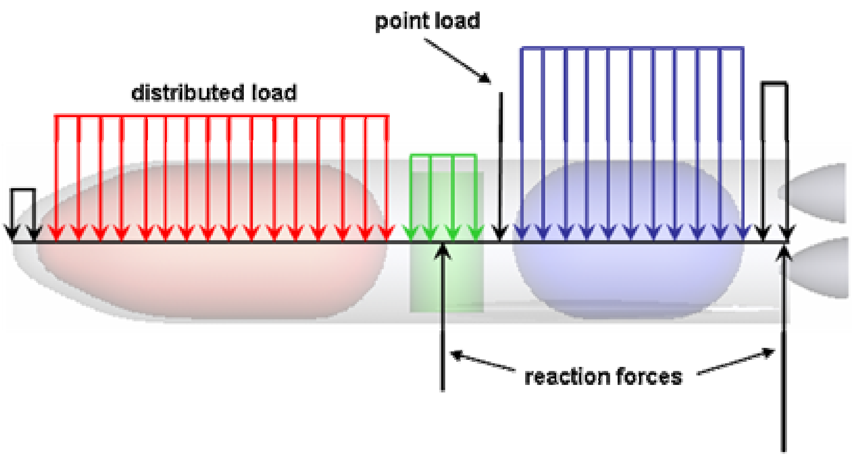

Figure 2. Visual Representation of Vehicle Weight Definition.

This methodology simulates liquid propellant contained in an integral tank structure arrangement. Also, the method does not analytically model the stress involved in the propellant tank end closures (i.e. hemispherical, elliptical). Instead an effective tank length is employed, which accounts for the distance of the tank end closures. The effective tank length for cylindrical tanks with end closures in the form of hemispherical or elliptical shape is equal to the tank barrel length plus one-third the depth of the end closures, as illustrated in Figure 3.[5]

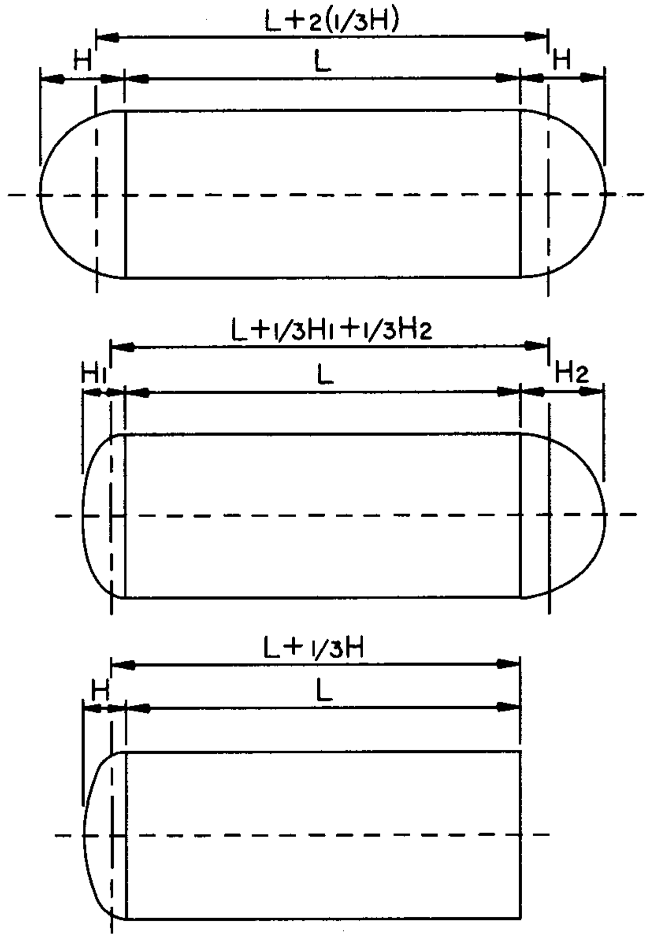

Figure 3. Effective Length of Cylindrical Tanks with Various End Closures
(Jawad, *Design of Plate & Shell Structures*, p. 376).

External Loads

After defining the inert masses and propellant masses on the beam approximation model of the vehicle, the next step is modeling the external loads experienced by the vehicle at the selected load conditions. The external stress resultants are determined on a station-by-station basis along the length of the fuselage. The three external loads considered are axial force, shear force, and bending moment. Calculation of the external loads involves the defined weights of the vehicle and account for the experienced accelerations and amount of propellant available at each load condition.

Load Conditions

Prior to determining the external loads, a set of load conditions that the vehicle will be subjected to during its trajectory are defined for the structural weight estimation. Some typical load conditions used are vehicle on the pad, liftoff, maximum dynamic pressure, maximum thrust, maximum axial acceleration, the product of maximum dynamic pressure and angle of attack, and reentry. Each defined load condition also provides the location of the two simple support reaction points along with the axial acceleration, normal acceleration, propellant ullage pressure, and percent of remaining fuel at the particular point in the trajectory. Information about the load condition may be acquired from a combination of sources and programs. For the verification examples presented later within the study, the information required for each load condition was obtained from POST – a trajectory optimization program.[6]

The reaction loads determined at the simple support locations are essential in the calculation of the shear force and bending moment over the length of the vehicle, which are in a normal direction to the vehicle beam approximation model. In order to determine the axial force, the weight is distributed axially along an unsupported (free) beam model of the vehicle. Unlike the external stress resultants modeled using the simple support beam model, the calculation of the axial force does not depend on the reaction loads. Therefore the locations of the supports on vertically launched vehicles at liftoff are not important because the normal acceleration at this condition is essentially zero. After liftoff when the vehicle initiates the pitch-over maneuver of its trajectory, the locations of the reaction loads become important because the normal acceleration is no longer negligible. The locations of the simple support are determined by the user after taking into consideration such factors as the air-loading, wing loading, vehicle weight distribution, and gimbal point position of the engine at a particular point within the trajectory.

Center of Gravity

With the load conditions defined, the process to ascertain the external loads begins by determining the simple support reaction loads. First the location of the vehicle's center of gravity is calculated by the following:

$$cg = \frac{\sum_{i=1}^{n} W_i d_i}{\sum_{i=1}^{n} W_i} \tag{2}$$

where n is the total number of component masses defined. Utilizing Newton's 1st Law that *the resultant force acting on a particle is zero*[7], the simple support reaction loads for each load condition are calculated by summing the moments about second location to determine the first reaction load, and then summing the forces in the y-direction to determine the second reaction load. Once the reaction loads are determined they are added to the vehicle weight definition. Since the accelerations and weight definition varies throughout the vehicle trajectory, the reaction load values are updated for each load condition.

Shear Force

For homogeneous materials, the combination of Hooke's law and the flexure formula with the definition of the radius of curvature results in the following relation for the curvature of a beam subjected to a bending moment (M)[8]:

$$\frac{1}{\rho_c} = \frac{M}{EI} \tag{3}$$

where ρ_c is the radius of curvature. From calculus, the curvature of a plane curve is expressed mathematically as[9]:

$$\frac{1}{\rho_c} = \frac{d^2y/dx^2}{\left[1+\left(dy/dx\right)^2\right]^{3/2}} \tag{4}$$

where the y is the deflection of the beam at any point x along its length. The slope of the beam at any point x is

$$\theta_s = \frac{dy}{dx} \tag{5}$$

For many problems in bending the slope is very small, which allows the denominator of eq. (4) to be taken as unity. Therefore substituting eq. (3) into eq. (4) yields the following equation that relates the bending moment to the deflection of the beam:

$$\frac{M}{EI} = \frac{d^2y}{dx^2} \tag{6}$$

From Euler-Bernoulli beam theory, the equilibrium equations for a beam subjected to pure bending give the following relations for shear force (V) and normally distributed loading (w_y) at a point on the beam[10]:

$$-w_y = \frac{dV}{dx} \tag{7}$$

$$V = \frac{dM}{dx} \tag{8}$$

By successfully differentiating eq. (6) and substituting into eq. (7) and (8) yields the following:

$$\frac{V}{EI} = \frac{d^3 y}{dx^3} \tag{9}$$

$$\frac{-w_y}{EI} = \frac{d^4 y}{dx^4} \tag{10}$$

The combination of eq. (9) and (10) yields eq. (7), and the integration of the distributed load in this equation yields the shear load, as defined by eq. (11)

$$V = -\int w_y dx \tag{11}$$

Following this fundamental structural analysis principle, the approximate integration of the distributed load of the defined component weights and the reaction loads station-by-station along the length of the fuselage yields the shear load at each station. Since the distance between each station along the fuselage, Δx, is relatively small compared to the overall vehicle length, the discretized technique is accurately determines the shear load over the vehicle. The distance between each fuselage station for this study was one inch. The discretized form of eq. (11) is

$$V = -\int w_y \Delta x \tag{12}$$

The normal acceleration for each load condition is also applied at each station to transform the distributed weight to the normal distributed load. Also, the percentage of propellant is applied to the propellant weights at the associated tank fuselage stations for each load condition. The accuracy of the discretized method versus the theoretical method in predicting the shear force of a cantilevered beam with an end load and a simply supported beam under uniform load are presented in Figures 4 and 5, respectively.

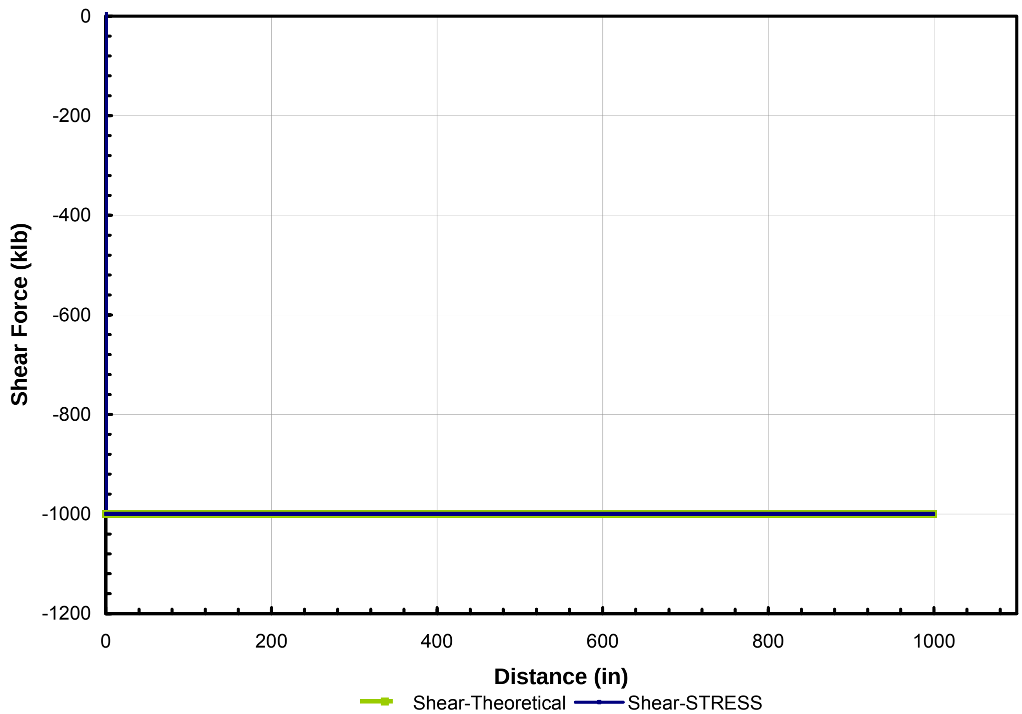

Figure 4. Shear Force Accuracy of Discretized vs. Theoretical Method for End Loaded Cantilevered Beam

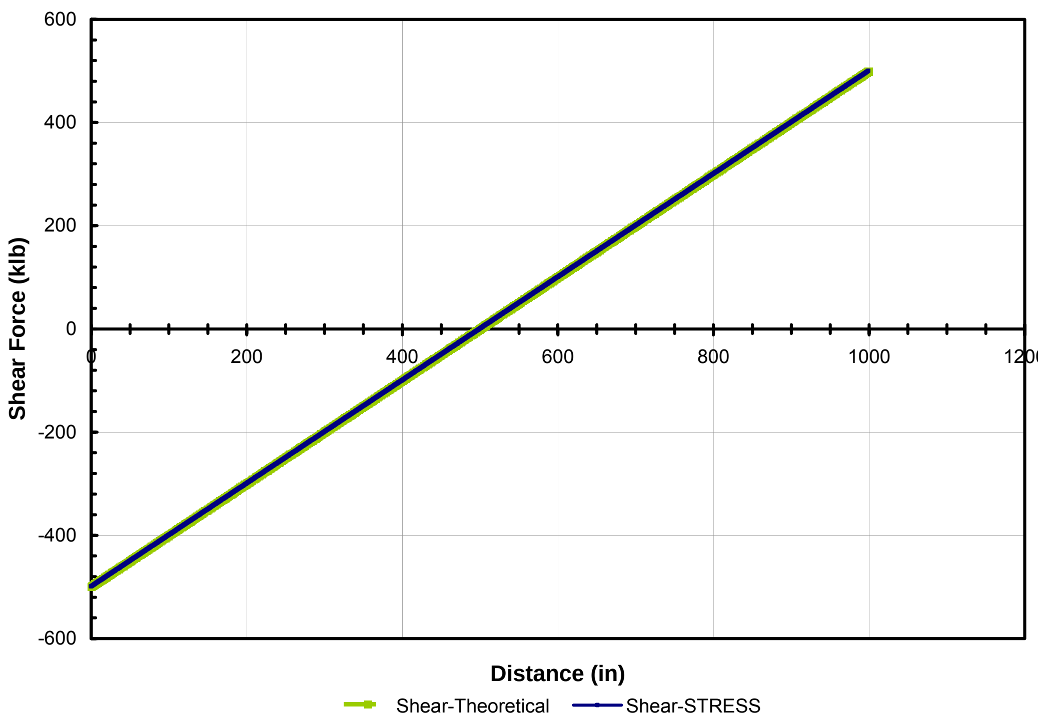

Figure 5. Shear Force Accuracy of Discretized vs. Theoretical Method for Uniformly Loaded Simple Support Beam

Bending Moment

Euler-Bernoulli equilibrium equations for a beam subjected to pure bending eq. (8) show that the integration of the shear force will result in the bending moment. By following the same procedure used for the shear load, the approximate integration of the shear load station-by-station along the fuselage length yields the bending moment at each fuselage station. The discretized form of eq. (8) is

$$M = \int V \Delta x \tag{13}$$

The accuracy of the discretized method versus the theoretical method in predicting the bending moment of a simply supported beam under uniform load and a cantilevered beam with an end load are presented in Figures 6 and 7, respectively.

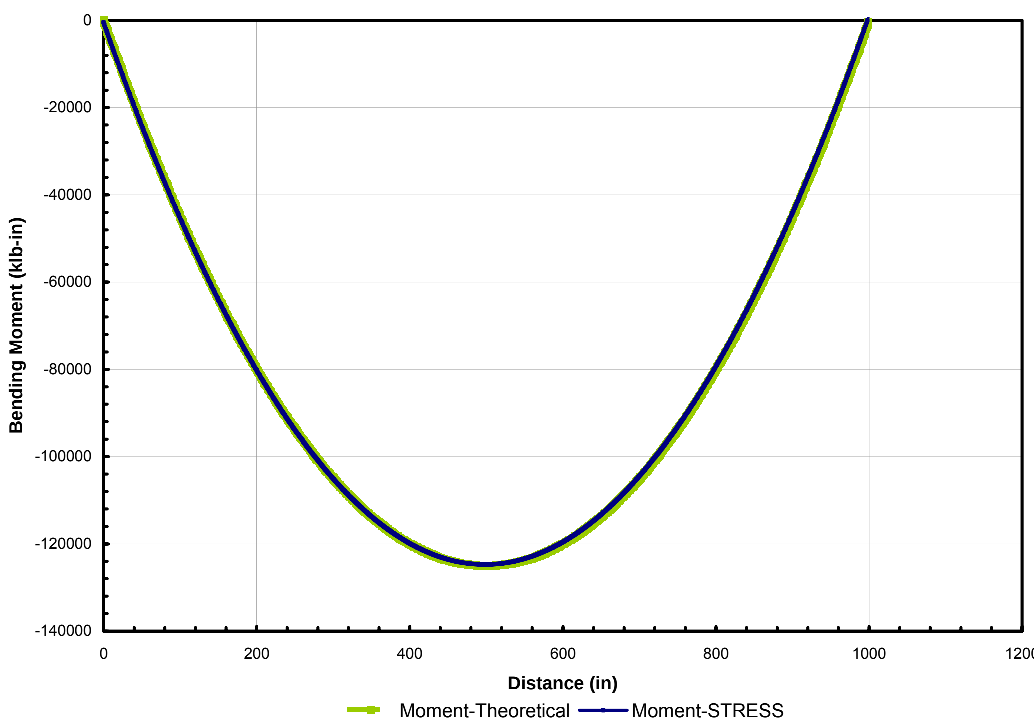

Figure 6. Bending Moment Accuracy of Discretized vs. Theoretical Method for Uniformly Loaded Simple Support Beam

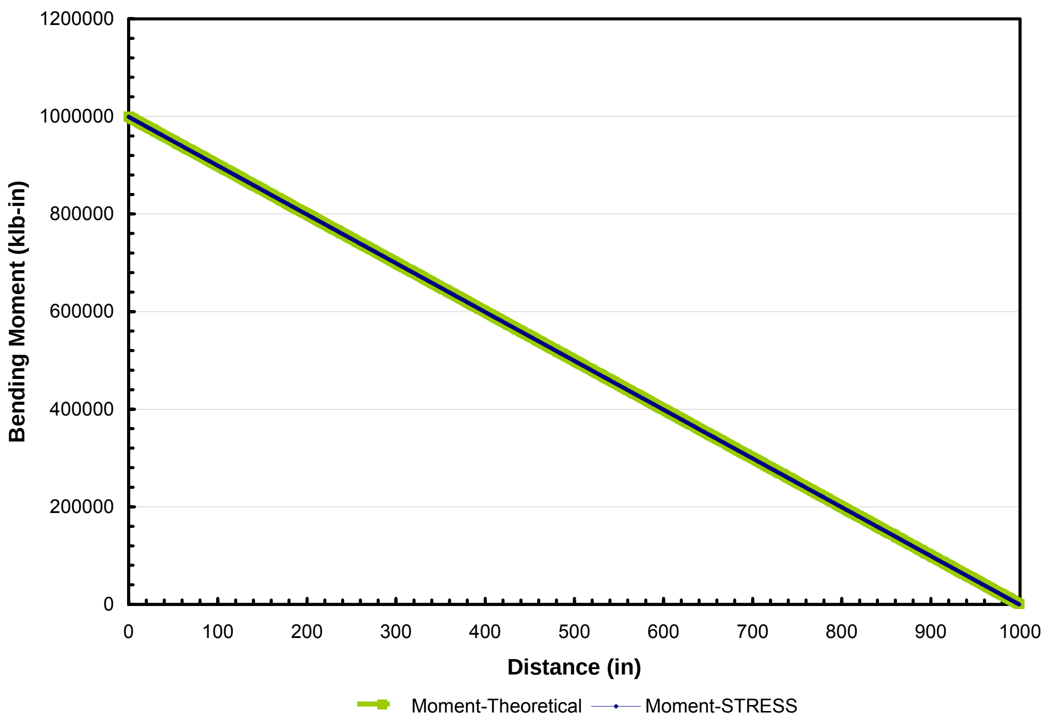

Figure 7. Bending Moment Accuracy of Discretized vs. Theoretical Method for End Loaded Cantilevered Beam

Axial Force

From Euler-Bernoulli beam theory, the equilibrium equations for a beam subjected to axial loads give the following relations for axial load and axially distributed loading at a point on the beam[10]:

$$-w_x = \frac{dP}{dx} \tag{14}$$

Therefore the integration of the distributed load in eq. (14) yields the axial load:

$$P = \int -w_x dx \tag{15}$$

Following the same procedure for the shear force and bending moment, the approximate integration of the axial load station-by-station along the fuselage length yields the axial load at each fuselage station. The discretized form of eq. (15) is

$$P = \int -w_x \Delta x \tag{16}$$

The accuracy of the discretized method versus the theoretical method in predicting the axial force of a cantilevered beam with under uniform load is presented in Figure 8.

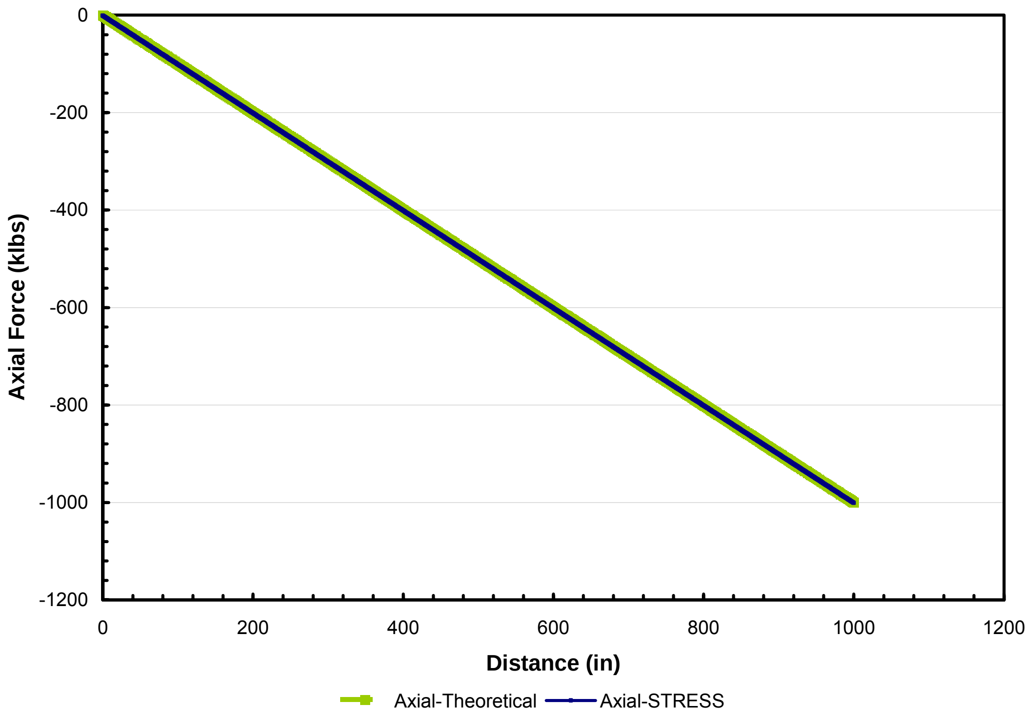

Figure 8. Axial Force Accuracy of Discretized vs. Theoretical Method for Uniform Loaded Cantilevered Beam

Also, the axial force contributions for the propellants are not added to the integral tank axial force calculation until the end of the tank is reached due to the inability of rest of the tank to withstand axial loads[4]. There is no structure within the tank that can resist the axial motion of the fluid except for the bulkheads at the ends of the tank. The reaction onto the axial load by the tank increases as the fluid becomes closer to the bulkhead, and also increases along the meridian of the bulkhead. Instead of modeling the distribution of the fluid axial load along the distance of the tank, the total axial load contribution from the propellant is loaded at the end of the tank to more accurately model the weight sustained by the tank bulkheads and reduce the complexity of the analysis.

Running Loads

Running loads are the internal shell stress resultants used to size the thickness of the shell for the fuselage and its associated components. Running loads are calculated by the product of the shell thickness and the stresses derived from the external loads (bending moment, axial force, and shear force) and the internal tank pressure (ullage pressure and head pressure). The running loads in the fuselage shell are a function of axial and circumferential position and are determined on a station-by-station basis. The top and bottom sections of the shell are loaded mainly in bending stress, the side sections are loaded mainly in shear stress, and the axial stress is loaded over the entire cross section.

Since the axial stress is loaded over the entire cross section of the shell, the axial stress contribution to the total longitudinal running load is determined by the product of the axial stress and the shell thickness:

$$N_{xaxial} = \sigma_{axial} t_s = \frac{P}{A} t_s = \frac{P}{P_{ell} t_s} t_s = \frac{P}{P_{ell}} \tag{17}$$

where the axial stress is the quotient of the axial load and the cross-sectional area of the shell, which is the product of the shell thickness and the elliptical perimeter of the section as defined in eq. (1).

The bending stress contribution to the axial running load is determined by the product of the bending stress and the shell thickness. The bending stress is calculated using the flexure formula:

$$\sigma_{bend} = \frac{Mc}{I_y} \tag{18}$$

where the distance farthest from the neutral axis along the y-axis (c) is the semi-minor axis and the moment of inertia for a thin-walled elliptical cross-section is determined by the following [11]:

$$I_y = \frac{\pi}{4} t_s b^2 (b + 3a) \tag{19}$$

Therefore the bending stress contribution to the axial running load is determined by the following:

$$N_{x\,bend} = \sigma_{bend} t_s = \frac{Mc}{\frac{\pi}{4} b^2 (b + 3a)} \tag{20}$$

The actual shear stress varies over an elliptical section, but since the maximum value of the shear stress is at the side of the section, the maximum shear stress for an elliptical shell section is determined by the following:

$$\tau_{xy\max} = \frac{2V}{A} \tag{21}$$

The distribution of shear stress over the elliptical cross section is presented in Figure 9.

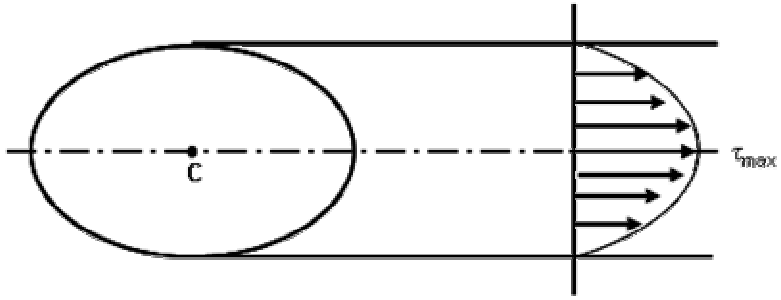

Figure 9. Shear Stress Distribution over an Elliptical Section

The shear running load is determined by the product of the maximum shear stress and the shell thickness. Since the cross-sectional area of the shell is the product of the thickness and perimeter, the shear running load is calculated by the following:

$$N_{xy} = \frac{2V}{P} \tag{22}$$

The internal tank pressure has a contribution to the axial running load and also has the only contribution to the circumferential running load. Two pressures contribute to the running loads: ullage pressure and head pressure. Ullage pressure is the gauge pressure that is developed by the pressurization of the propellant within the tank. [8] The weight of the pressurant is assumed negligible.[8] The ullage pressure is defined for each load condition. Head pressure is the pressure based on the height level of the propellant within the tank, and it is determined by the following:

$$p_{head} = \rho_p g_{axial} h \tag{23}$$

where the height level (h) and axial acceleration (g_{axial}) for the head pressure are defined for each load condition. The distribution of the head pressure, which is also known as hydrostatic distribution, shows that in an incompressible fluid at rest the pressure varies linearly with depth. Therefore the pressure must increase with depth in order to *hold up* the fluid above it.[23]

The normal stress in the hoop (circumferential) and axial (longitudinal) directions for a cylindrical tank with a circular cross section are determined by the following:

$$\sigma_h = \frac{pr}{t_s} \tag{24}$$

$$\sigma_l = \frac{pr}{2t_s} \tag{25}$$

Instead of restricting the fuselage cross-sectional shape to a circle, this analytical method utilizes a general elliptical cross section which allows for both elliptical and circular sections. From membrane stresses in pressure vessel theory, the radius of curvature for the elliptical cross section can replace the circular radius in the calculation of the hoop and axial pressure stresses.[12] Using calculus, the radius of curvature of an ellipse as a function of angle is determined by the following[13]:

$$R_t = \frac{\left(a^2 \sin^2 \theta + b^2 \cos^2 \theta\right)^{3/2}}{ab} \tag{26}$$

Since the radius of curvature varies at different points along the edge of the cross section, the following criteria was developed to select the angle for the maximum radius of curvature value based on the lengths of the semi-major and semi-minor axes:

- for a < b, $R_{t,max}$ is at 0° and 180°
- for a > b, $R_{t,max}$ is at 90°
- for a = b, $R_{t,max}$ = a = b = r (circular section)

Replacement of the radius with the radius of curvature for the determination of the hoop and axial pressure stresses are presented by the following:

$$\sigma_h = \frac{pR_t}{t_s} \tag{27}$$

$$\sigma_l = \frac{pR_t}{2t_s} \tag{28}$$

The contribution of the tank ullage and head pressures to the longitudinal and circumferential running loads are calculated by the product of the shell thickness and the axial and hoop stress, as shown below:

$$N_{xullage} = \sigma_{l\,ullage} t_s = \frac{p_{ullage} R_t}{2} \tag{29}$$

$$N_{xhead} = \sigma_{l\,head} t_s = \frac{p_{head} R_t}{2} \tag{30}$$

$$N_{yullage} = \sigma_{h\,ullage} t_s = p_{ullage} R_t \tag{31}$$

$$N_{yhead} = \sigma_{h\,head} t_s = p_{head} R_t \tag{32}$$

After obtaining the individual contributions from the external loads and internal tank pressures, the total longitudinal, circumferential, and transverse running loads are determined by the following:

$$N_x = N_{xbend} + N_{xaxial} + N_{xullage} + N_{xhead} \tag{27}$$

$$N_y = N_{yullage} + N_{yhead} \tag{28}$$

$$N_{xy} = \frac{2V}{P} \tag{22}$$

The total axial, hoop, and shear running loads are calculated station-by-station along the fuselage for each load condition. The maximum values of the axial, hoop, and shear running loads from all of the load cases at each station along the fuselage length are used to determine the shell material thickness based on the *worst-case* scenario. This ensures that the vehicle structure will be able to withstand all of the load conditions throughout the trajectory. For each station the maximum bending moment about the neutral axis (y-axis) for an elliptical section occurs at 90° and 270°[12], the maximum bending shear stress for the section occurs at 0° and 180°[9], and the axial stress remains constant over the entire cross section. The distribution of bending moment and shear stress along the elliptical cross section, which reflect the location of the maximum values, are displayed in Figures 9 and #, respectively.

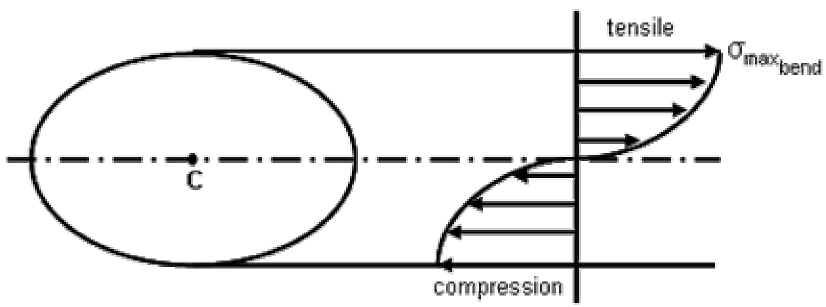

Figure 10. Bending Moment Distribution over an Elliptical Section

Therefore the *worse-case* scenario shell will be modeled as the maximum thickness corresponding to the maximum shear stress and bending moment at their respective locations to prevent structural failure. A factor of safety of 1.5 is also applied to each running load.

Structural Sizing

The maximum running loads determined at each fuselage station are used to calculate the amount of shell material required to preclude failure. The most critical point of the shell thickness is assumed to be the outermost location of the circumference, which is the position of the maximum stress experienced. The failure modes considered are ultimate strength, yield strength, and buckling. A material minimum gage restriction is also imposed as a final failure criterion. The shell thickness is selected as the maximum thickness from the failure modes at each fuselage station.

Ultimate Strength Failure

Ultimate strength failure is based on the maximum principal stress and describes when a material fails suddenly by fracture without apparent yielding.[8] According to the maximum-normal-stress theory, the failure of a brittle material will occur when the maximum principal stress in the material reaches a limiting value that is equal to the ultimate tensile strength of the material (σ_{UTS}).[8] The equation for the maximum principal stress is given by the following:

$$N_1 = \frac{N_x + N_y}{2} + \sqrt{\left(\frac{N_x - N_y}{2}\right)^2 + N_{xy}{}^2} \tag{29}$$

The equivalent isotropic thickness of the shell material is determined by the following:

$$N_1 = \sigma_{UTS} t_{s,UTS} \tag{30}$$

$$t_{s,UTS} = \frac{N_1}{\sigma_{UTS}} \tag{31}$$

Yield Strength Failure

For a homogeneous, isotropic material subjected to a general three-dimensional state of stress, the equivalent stress in the material is defined by the following equation:

$$\sigma_{eq} = \left[\sigma_x{}^2 + \sigma_y{}^2 + \sigma_z{}^2 - \sigma_y\sigma_z - \sigma_z\sigma_x - \sigma_x\sigma_y + 3\left(\tau_{yz}{}^2 + \tau_{xz}{}^2 + \tau_{xy}{}^2\right)\right]^{1/2} \tag{32}$$

The equivalent running load is defined by the following equation:

$$N_{eq} = \left[N_x{}^2 + N_y{}^2 + N_z{}^2 - N_yN_z - N_zN_x - N_xN_y + 3\left(N_{yz}{}^2 + N_{xz}{}^2 + N_{xy}{}^2\right)\right]^{1/2} \tag{33}$$

Since the in-plane stress resultant normal to the plane (N_z) is assumed negligible, eq. (33) is reduced to the following equation:

$$N_{eq} = \left[N_x{}^2 + N_y{}^2 - N_xN_y + 3\left(N_{xy}{}^2\right)\right]^{1/2} \tag{34}$$

The Von-Mises strength criterion postulates that under combined loading, the safe stress level is such that the equivalent stress is smaller than the allowable stress, which is the material yield strength.

$$\sigma_{eq} \le \sigma_{yield} \tag{35}$$

The equivalent shell material thickness based on the failure criteria is determined by the following:

$$N_{eq} \le \sigma_{yield} t_{s,YS} \tag{36}$$

$$t_{s,YS} \ge \frac{N_{eq}}{\sigma_{yield}} \tag{37}$$

In order to minimize the shell material weight, the shell thickness for the yield strength failure is equal to the quotient of the equivalent running load and the material yield stress.

Minimum Gage Restriction

The minimum gage restriction is used to enforce that the material thickness not be smaller than the minimum material thickness. The equivalent shell material thickness based on the minimum gage restriction is determined by the following:

$$t_{s,mg} = K_{mg} t_{mg} \tag{38}$$

where K_{mg} is the minimum gage parameter that relates the shell thickness to the minimum material thickness. This parameter is derived from the fuselage skin and shell arrangement for various stiffened shell configurations typically used in aerospace vehicles by Mark Ardema and company in *Analytical Fuselage and Wing Weight Estimation of Transport Aircraft*.[1]

Buckling Failure

The maximum running loads determined at each fuselage station are used to size both the fuselage stiffened shell and general-stability frames required to preclude buckling failure. The calculations to size the fuselage shell assume a wide column behavior of the shell, and the required stability ring frames are sized using the Shanley criterion.[14]

Stiffened Shell

The fuselage is modeled as a long, wide column with a (length-to-width ratio ≥ 10). For shell type structures, such as a fuselage, a large portion of the material must resist axial loads caused by bending. Given that the material is also used to form the shell, the column must be spread out over a considerable width. Since the width is many times larger than the column's thickness, buckling can occur only in a direction normal to the plane of the column. If further assumed that the edges are unsupported or to the effect that such support is negligible, the bending stiffness across its width may be neglected. Therefore the wide column may be thought of as a series of individual columns placed side by side and equally loaded.[14]

Minimum weight equations for wide column stiffened shells were determined by Crawford and Burns in 1963.[15] The form of the equation is the following:

$$\frac{N_x}{LE} = \varepsilon\left(\frac{t_s}{L}\right)^m \tag{39}$$

where ε is the shell buckling efficiency, *m* is the equation exponent, *L* is the frame spacing, and *E* is the modulus of elasticity for the shell material. The shell buckling efficiency and equation exponent are a function of certain proportions of the stiffened shell configurations under consideration. For each equation, these geometric proportions have been varied in order to obtain a maximum shell buckling efficiency, which will in turn result in a minimum shell thickness and a minimum weight for the shell.[15] All of the shell configurations used within this study has an equation exponent equal to 2, which then solving for the shell thickness leads to the following equation:

$$t_{s,B} = \sqrt{\frac{N_x L}{E\varepsilon}} \tag{40}$$

The shell buckling efficiency and equation exponent values are given for each shell configuration in Table I.

Table I. Stiffened Shell Configuration Factors for Wide Column Shell.

Shell Configuration	ε	*m*	K_{mg}
Simple unflanged integrally stiffened	0.656	2	2.463
Z-stiffened	0.911	2	2.475
Truss-core sandwich	0.605	2	4.310

Stability Frame

In addition to the stiffened shell, ring frames are sized to prevent general instability failure of the fuselage using the Shanley criterion. The Shanley criterion is based on the principle that the frames act as elastic supports for the wide column shell.[1] To predict the general instability failure that could occur with the stiffened-shell segment between two frames, Shanley associated the behavior of the structural system to the fundamental model of general instability failure – two hinged bars supported by two springs, as displayed in Figure 11.

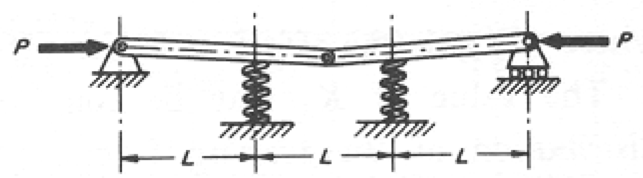

Figure 11. Model for General Instability Failure
(Shanley, *Weight Strength Analysis of Aircraft Structures,* p. 65).

By modeling the shell segment as the hinged bars and the frames as the two springs located midway between each bar, Shanley derived the following expression to determine the required frame stiffness to prevent general instability.[14]

$$(EI)_f = \frac{C_f M D^2}{L} \tag{41}$$

The experimentally obtained value of the Shanley constant, C_f, is 1/16,000.[14] By solving the expression for the Shanley's constant, which remains constant for any cross-sectional shape, the following equation is derived[14]:

$$C_f = \frac{(EI)_f L}{MD^2} \tag{42}$$

Deriving the expression based on the Shanley constant permits the frame problem to be handled independently of the parameters involved with the sizing the stiffened shell.

Shanley also defines the frame weight per inch length by the following expression:

$$W_f' = \frac{\pi k_c D^2 M^{1/2} \rho_f}{L^{3/2}} \left(\frac{C_f}{k_f E_f} \right)^{1/2} \tag{43}$$

where k_f is frame stiffness coefficient, k_c is the shape correction factor for circumference of non-circular shell cross-sections, and E_f is the modulus of elasticity for the frame. The frame stiffness coefficient is determined from the quotient of the moment of inertia of the frame cross-section and the cross-sectional area of the frame.

$$k_f = \frac{I_f}{A_f^{\,2}} \tag{44}$$

Manufacturers generally use I-beam and C-shape section beams for stability ring frames within the vehicle fuselage. This methodology uses a C-shape section beam defined by Shanley for fuselage ring frames.[14] The dimensions and shape of the beam are presented in Figure 12.

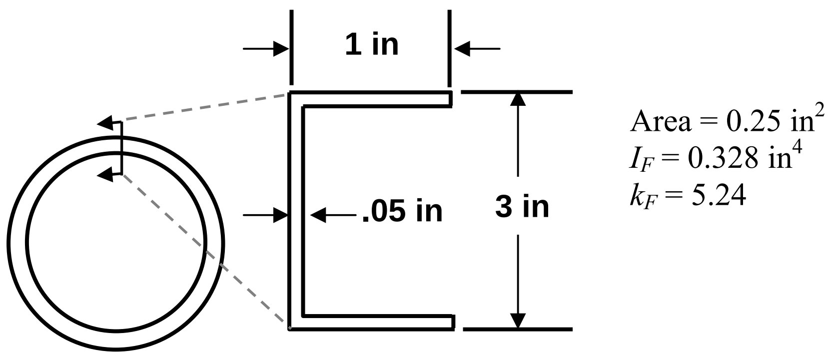

Figure 12. Shape and Dimensions of Frame Cross Section.

The shape correction factor for non-circular cross-sections allows for the application of the Shanley formulas, which are based on circular cross sections, to non-circular cross sections. The factor is calculated by dividing the perimeter of the non-circular section by the product of pi and the depth of the cross-section (D).

$$k_c = \frac{P_{non-circular}}{\pi D} \tag{45}$$

The depth of the cross-section is the diameter of a circular section and the larger of the major or minor axes for an elliptical section.

Dividing the frame unit weight by the frame density yields the ring frame cross-sectional area with respect to the fuselage cross section.

$$A_f = \frac{\pi k_c D^2 M^{1/2}}{L^{3/2}} \left(\frac{C_f}{k_f E_f} \right)^{1/2} \tag{46}$$

Equating the expression of the ring frame cross-sectional area to the general cross-sectional area of a circular shell (the product of the section perimeter and the frame thickness) and solving for the thickness results in the *smeared* equivalent thickness of the frames.

$$t_f = \frac{k_c D^2}{2} \sqrt{\frac{C_f \pi N_x}{L^3 k_f E_f}} \tag{47}$$

Assuming that the shell is buckling critical, the total thickness is the sum of the buckling shell thickness and the *smeared* frame thickness.

$$t = t_{s,b} + t_f = \sqrt{\frac{N_x L}{E\varepsilon}} + \frac{k_c D^2}{2}\sqrt{\frac{C_f \pi N_x}{L^3 k_f E_f}} \tag{48}$$

Minimizing the total thickness with respect to the frame spacing and solving for the frame spacing yields an expression for the frame spacing that is a function of the coefficient parameters and cross-section depth.

$$L = \left(\frac{3}{2} k_c D^2 \left(\frac{\rho_f}{\rho_s}\right)\sqrt{\frac{C_f \pi E_s \varepsilon}{k_f E_f}}\right)^{1/2} \tag{49}$$

Typically the frames used to support general stability and the fuselage shell are made of the same material. In special cases, major frames that are used to withstand the impact of large stress loads throughout the vehicle (i.e. landing gear, thrust structure) might be made of steel or other types of materials. This study assumes that the shell and frame materials are the same.

Structural Shell and Frame Sizing

The fuselage shell must satisfy all failure criteria at each station. The shell thickness was determined by selecting the maximum thickness according to the ultimate strength, yield strength, buckling, and minimum gage failure.

$$t_s = \max\left(t_{s,UTS}, t_{s,YS}, t_{s,B}, t_{s,mg}\right)$$

If $t_s = t_{s,B}$, the shell structure is buckling critical, and the equivalent isotropic thickness of the frames (t_f) is computed using the given equation from Shanley. If $t_s > t_{s,B}$, the shell structure is not buckling critical at the optimum frame sizing. The frames are resized to make the selected shell thickness buckling critical ($t_s = t_{s,B}$). New frame spacing is computed using the shell buckling thickness equation as

$$L = \frac{t_s^{\,2} E_s \varepsilon}{N_x} \tag{50}$$

This new frame spacing is used with the frame thickness equation to resize the frame.

The total thickness of the fuselage structure is calculated by the summation of the shell and *smeared* frame thicknesses. The total ideal fuselage structural weight is determined by the summation of the shell and frame weight at each station along the length of the fuselage.

$$W_T = \sum P_{ell\,i}\left(\rho_s t_{s\,i} + \rho_f t_{f\,i}\right)\Delta x_i \tag{51}$$

where the quantities subscripted i depend on position along the length of the fuselage, and distance between each station (Δx_i) is one inch.

Implementation of Analytical Methodology into GT-STRESS Computer Program

The methodology developed from fundamental beam structural analysis was implemented into a computer program to allow for the rapid estimation of the load-bearing structural weight of the launch vehicle fuselage and its associated components. Rapid approximation of the vehicle structural weight permits this design tool is useful for conceptual vehicle design studies.

The Georgia Tech Structural Tool for the Rapid Estimation of Shell Sizes (GT-STRESS) is a C++ constructed computer program that utilizes the previously described fundamental beam structural analysis to calculate the required running loads for sizing the fuselage shell and frames based on selected material and shell structure properties. From the determined shell thickness and selected material properties, the structural weight is calculated. The program simulates a launch vehicle fuselage fueled by liquid propellant contained in an integral tank structure arrangement.

The information input and basic operation of GT-STRESS are derived from RL, a computer program to calculate fuselage running loads, which was developed by Jeff Cerro, formerly of Lockheed Martin Engineering & Science Services.[4] GT-STRESS accepts a specified input text file that describes the geometry, preliminary subsystem weights, and the load conditions experienced by the vehicle. After operation the program computes the fuselage structure weight and other vehicle component weights (i.e. propellant tanks, interstages) as specified in the input file. Along with the resulting structural weight, the program will also generate output files that contain the summary of the information received from the input file, external stress resultants over the vehicle length for each load condition, running loads for the overall vehicle, shell and frame thickness for the overall vehicle, and a structural weight breakdown based on fuselage and structural components.

GT-STRESS Input File

The program input for GT-STRESS is a text input file derived from the RL input format that describes the geometry, preliminary subsystem weights, and the load conditions experienced by the vehicle. Keywords located within the input file are utilized by the program to recognize the relevant information required to run the program. All of the data within the input file is free field format (separate values on a line by whitespace). The first line within the file is a onehundred character max descriptive title. The second line beginning with the keyword *oal* is the overall fuselage length in inches.

The next section is the vehicle geometry section. The geometry definition begins with the keyword *geom* and ends with the keyword *end_geom*. Between these two keywords are the input for the *x* location, semi-major axis, and semi-minor axis for each elliptical cross section used to define the vehicles geometry. Each line has the geometric information for one cross section, and all of the parameters are given in inches. The minimum and maximum amount of sections defined within the input file are two and ten, respectively. The initial *x* location must be at zero inches and the final *x*-location must be at the value of the overall fuselage length. An example of the geometry definition section from the input file is listed in Table II.

Table II. Example GT-STRESS Input File Geometry Definition

```
geom
  0     1     1
  160   85    85
  600   200   200
  1800  200   200
  2000  100   100
end_geom
```

Preliminary vehicle weights are defined in the next section. The section begins with the keyword *weights* and ends with the keyword *end_weights*. For each line within the weight section, a one word description is entered for each uniformly distributed weight. Following the description is the beginning *x*-location of the load (in inches), then the ending location, and then the total weight in pounds to be distributed over the given range. For point loads the end location equals the beginning load location. Propellant loads have a slightly different input that allows the program to obtain additional propellant property information. For propellant loads, the keyword *propellant* is entered at the beginning of the line, followed by the beginning load location, ending load location, and weight. Following the weight value is a descriptor of the propellant type. The propellant type descriptor instructs the program to select and store the proper propellant density from a text file database that is external to the GT-STRESS program. Head pressure loads contribution to the overall bending and axial forces within the tank area of the fuselage are computed using the selected propellant density. Note that the structural weight for the propellant tanks are entered under separate descriptors in order to allow their weight to be used as feedback variables for vehicle weight convergence without including the propellant weight. GT-STRESS operation limits the maximum amount of weights defined within the input file to thirty-five in order to minimize the computational effort of the program and ensure that the time required to determine the structure weight is kept within a few minutes.

The following section identifies the vehicle components sized by GT-STRESS. Structural components are subsystem components of the fuselage structure selected from the weight definition to have their actual weight value calculated and replaced into the weight definition. The section begins with the keyword *structure* and ends with the keyword *end_structure*. Each line contains the one word description from the *weights* section that describes the structural component. GT-STRESS uses these components as feedback variables to converge the vehicle structural weight by fixed point iteration (FPI). Weight values defined for each of these components within the *weights* section are perceived as initial guess values. After the first analysis of the vehicle by GT-STRESS, these initial weight values are replaced by the structural weight calculated using the analytical method within the program. Once the weight values are replaced, GT-STRESS runs another iteration of analysis of the vehicle and calculates new values of the structural components weight and vehicle weight based on the new initial values taken from the last iteration. This iteration continues until the difference between the previous and present values of the total vehicle structural weight reaches absolute convergence. The absolute convergence criteria programmed within GT-STRESS is that the difference between the vehicle weight values is less than or equal to 1×10^{-4} pounds. After the vehicle structural weight has converged, weight values of the structural components are recalculated and included in an output file by the program. A flow chart of the convergence process to obtain the structural component weight is displayed in Figure 13.

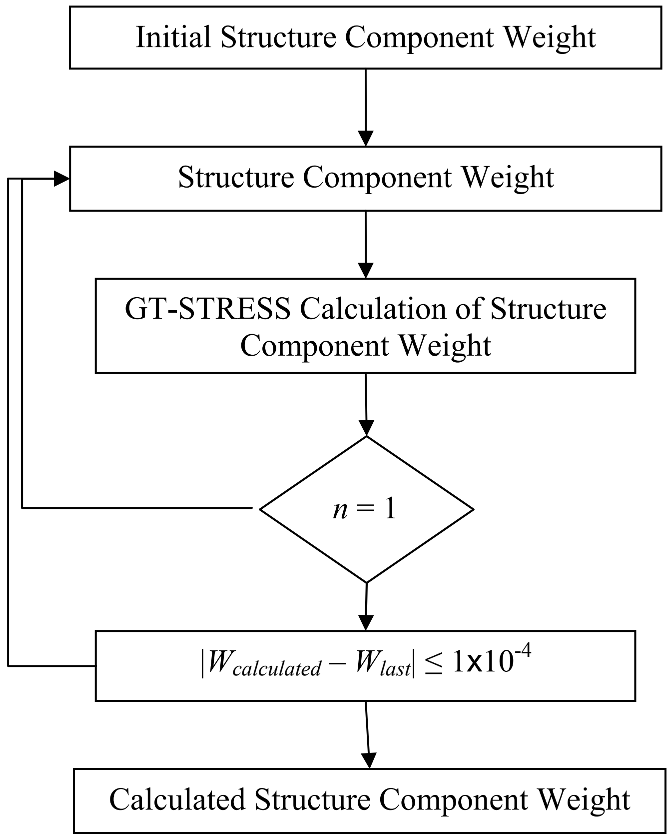

Figure 13. Convergence Process for Determining Structure Component Weight.

The shell and frame materials along the length of the vehicle are defined in the next section. The section begins with the keyword *material* and ends with the keyword *end_material*. The first line in this section beginning with the keyword *default_shell* identifies the default shell configuration for the fuselage, which would be one of the three stiffened shell configurations defined in Table I. The second line beginning with the keyword *default_mat*, is the default material selected for the fuselage. Both the shell and frame are composed of the same material within the program. GT-STRESS uses the default shell configuration and material to calculate the thickness and weight of the shell and frame at each station where the material and shell configuration is not specifically defined. Each following line until the end of the section is describes the material and shell structure types that are different from the default selections along the length of the fuselage. The line begins with a one-word material description that GT-STRESS uses to locate the associated properties of the material defined within a text file database external to the program. A variety of homogeneous isotropic materials and a generic composite material defined within the database file. Following the material description is the beginning x-location of the material (in inches), then the ending location, and then a one-word description of the shell configuration type for the given range. The coefficient information for the shell configurations presented in Table I are hard coded into the GT-STRESS program and recognized by the associated keywords presented in Table III. Any discrepancy between the material or shell configuration descriptions in the input file and their recognition by GT-STRESS program will result in the replacement of their associated values with the values of the defaults defined in the input file. If there is any discrepancy between the default descriptions and their recognition by GT-STRESS, then their associated values will be replaced with the default values hard coded within GT-STRESS for aluminum and Z-stiffened shell configuration. An example of the material definition section from the input file is listed in Table IV.

Table III. GT-STRESS Keyword for Stiffened Shell Configurations.

Shell Configuration	GT-STRESS Keyword
Simple unflanged integrally stiffened	simple
Z-stiffened	z-stiffened
Truss-core sandwich	sandwich

Table IV. Example Material Definition Section of GT-STRESS Input File.

```
material
  default_shell z-stiffened
  default_mat   aluminum
  aluminum      180 200   z-stiffened
  other         250 300   z-stiffened
  beryllium     501 1000  z-stiffened
  titanium      1080 2000 z-stiffened
end_material
```

The final input section defines the load conditions experienced by the vehicle. Each load condition or loadcase is defined in its individual section. The section begins with the keyword *loadcase #*, where # is a sequential loadcase number beginning with 1 for the first load condition, and ends with *end_loadcase*. GT-STRESS is limited to a maximum of fifteen loadcases. Formatting for all of the loadcase sections are the same. A descriptive loadcase title of 80 characters is entered on the first line beginning with the keyword *title*. The locations of the two simple support reaction points are specified by the keywords *x1* and *x2*. Normal and axial accelerations for the load condition are specified in g's by the keywords *axial_accel* and *normal_accel*. The sixth line, which begins with the keyword *prop_ullage*, defines the propellant tank ullage pressure in psi for each of the propellants defined within the *weights* section. Following *prop_ullage*, each subsequent pressure value is associated with the order the propellant is defined within the weights section. The next line beginning with the keyword *pct_fueled* defines the percent of propellant remaining within the tanks at the particular load condition. Each subsequent percent value after the *pct_fueled* keyword is associated with the order the propellant is defined within the *weights* section. An example of the loadcase definition section from the input file is listed in Table V.

Table V. Example Loadcase Definition Section of GT-STRESS Input File.

```
loadcase 1
title             Liftoff
x1                160
x2                1440
axial_accel       1.32
normal_accel      0.5
prop_ullage       25 25
pct_fueled        100 100
end_loadcase
```

After the final loadcase is defined, the last line of the file ends with the *end_loadcase* keyword for the final loadcase. Any subsequent lines after this line will result in an error in the GT-STRESS and cause the program to not operate. An example GT-STRESS input file is located in Appendix A.

GT-STRESS Propellant and Material Property Files

The propellant densities used to calculate the head pressure load and the material properties used to size the fuselage shell and frame structures are located in text files that are external to the GT-STRESS program. The propellant and material text files are propellant.txt and material.txt, respectively. These files are placed into the same file directory as the GT-STRESS program executable, and the incapability of the program to locate these files will result in immediate termination of the program.

Located within the propellant text file is a database of typical liquid propellants[18] and HEDM-based propellants[19] used for launch vehicles and keyword descriptions used to identify these propellants. The propellant type descriptor within the *weights* section for a propellant is used to locate the appropriate density within the propellant file. If the propellant descriptor is not found within the file, GT-STRESS gives an error message and terminates the program immediately. The propellants and propellant descriptors within the default propellant file are defined within Table VI.[18, 19] The propellant text file is located in Appendix B.

Table VI. Propellant Keywords from Default Propellant Database.[18, 19]

Keyword	Propellant
LOX	Liquid Oxygen
LH2	Liquid Hydrogen
H2O2	Hydrogen Peroxide
N2O4	Nitrogen Textroxide
RP1	Rocket Fuel
N2H4	Hydrazine
MMH	Monomethyl Hydrazine
UDMH	Unsymmetrical Dimethyl Hydrazine
FL, F2	Liquid Flourine
CH4, METHANE	Methane
JP	Jet Fuel
QUAD	Quadricyclane(C7H8)
BCP	BCP(C6H8)
AFRL1	AFRL-1
CINCH	CINCH(C4H10N4)
OCTAD	Octadiyne(C8H10)

The material properties for the fuselage and its associated components are assumed isotropic and homogeneous, which also include a generic laminate and core configuration of an aerospace grade composite material. The materials database file contains keyword descriptions of each material along with their associated modulus of elasticity, density, ultimate tensile strength, yield strength, and minimum gage thickness. Material descriptions defined within the *material* section of the input file are used to identify the appropriate material properties within the material file. In the case that the material description given in the input file is not located within the file, GT-STRESS will use the properties of the default material. Yet if the default material description is not located within the default material file, GT-STRESS will output an error message of the situation to the screen and use the aluminum material properties that are hard coded into the program. The materials and material descriptors within the default materials file are defined within Table VII.[20] An abbreviated version of the default material text file is presented in Table VIII. The material text file is located in Appendix C.

Table VII. Material Keywords from Default Material Database

Keyword	Material
aluminum	Aluminum
titanium	Titanium
beryllium	Beryllium
magnesium	Magnesium
steel	Steel
composite	Aerospace Grade Carbon Fiber Epoxy Composite
al-li	Aluminum Lithium

Table VIII. Abbreviated Version of the Default Material Text File

```
Material    E(psi)     rho(lb/in^3)    UTS(psi)   YS(psi)    min gauge(in)
aluminum    10300000   0.101           67000      55000      0.0056
titanium    16000000   0.160           130000     124000     0.0075
beryllium   43900000   0.0666          53700      34800      0.0056
magnesium   6500000    0.064           39000      24000      0.0056
steel       29700000   0.284           108000     68200      0.0075
composite   27557171   0.065029        117481     76870      0.0375
al-li       11200000   0.0918          74000      65300      0.0056
```

Using the external files as a database for the material and propellant properties provides the ability for the addition and modification of material and propellant keywords and properties within the database without affecting the functionality of the program or changing the program source code.

GT-STRESS Program Operation and Output

At the execution, the GT-STRESS program prompts the user to enter the name of the input file, the root name of the output file, and the value of the convergence relaxation factor. After entering the relaxation factor value GT-STRESS starts operation by reading in the geometry, preliminary weight, material, and loadcase data from the input file. The program continues by initiating the analysis to determine the external loads and running loads required to size the shell and frame material and ascertain the fuselage structure weight.

After the first analysis of the vehicle by GT-STRESS, the initial weight values of the components defined in the *structure* section of the input file are replaced by the structural weight calculated using the analytical method within the program. Typically there are 3-5 structural components for each stage of an expendable liquid propellant launch vehicle and 5-10 components for reusable launch vehicles. Once the component weight values are replaced, GT-STRESS runs another iteration of analysis and calculates new values of the components weight and vehicle weight based on the new initial values taken from the last iteration. After each iteration GT-STRESS outputs the current calculated vehicle structural weight and iteration number to the screen. This fixed point iteration (FPI) process continues until the difference between the previous and present values of the total vehicle structural weight reaches absolute convergence.

If the convergence process of the vehicle becomes unstable or the value of the component initial masses are vastly different from the converged computed values, reaching convergence for the vehicle structural weight can require a larger amount of iterations. Therefore relaxation was integrated into the FPI process to introduce damping into the convergence process and improve the stability. A relaxation factor (α) is introduced into the feedback variables of the FPI process by the following expression:

$$W_{next} = \alpha W_{calculted} + (1-\alpha)W_{last} \tag{52}$$

where W_{last} is the component weight from the previous iteration, $W_{calculated}$ is the component weight from the current iteration, and W_{next} is the component weight value fed back to the weight definition. Relaxation essentially takes a weighted average value of the component weight calculated from the previous and present iterations and feeds back this value to the weight definition. These averaged values of the feedback variables allows the vehicle weight to reach convergence quicker for a stable problem with extreme initial masses or reach a happy medium for an unstable problem. The relaxation factor value is between 0 and 1. A value of zero will only feedback the initial component masses, a value of one will continue feeding back the recent calculated value for each iteration as the basic FPI process, and ½ is an average value. An equivalent Multidisciplinary Analysis (MDA) model of the program operation is presented in Figure 13.

After the vehicle structural weight has converged, weight values of the structural components are recalculated and a series of output files are generated by the program. The output files and explanations of their contents are presented in Table V.

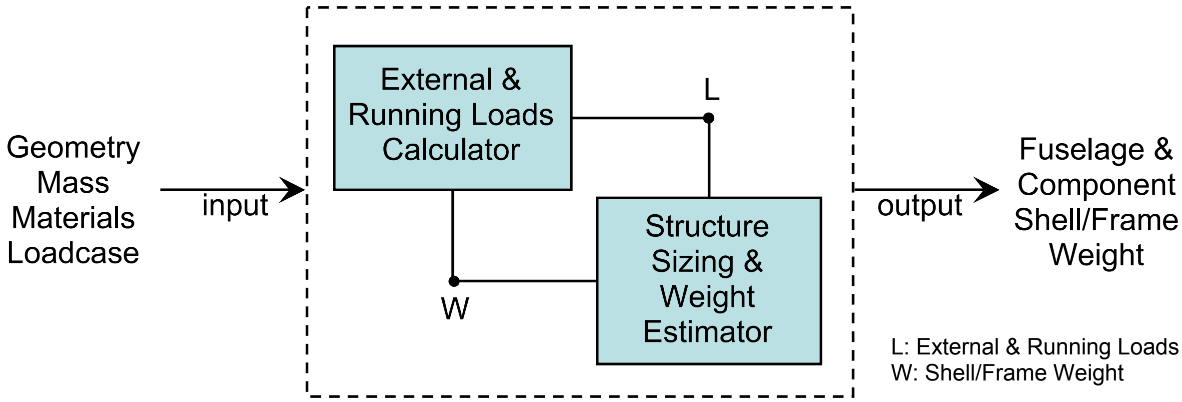

Figure 14. MDA Model of GT-STRESS Program Operation.

Table IX. GT-STRESS Output Files.

File Extension	Description
.cog	center of gravity information for each iteration
.dat	shell & frame weight by component and fuselage
.lod	external stress resultants and running loads over the vehicle length for each load condition
.out	shell & frame weight by component and fuselage for each iteration
.siz	shell and frame thickness for the overall vehicle
.sum	summary of the information received from the input file

Verification and Correlation with Existing Launch Vehicle Components

The analytical methodology for determining the structural weight of the fuselage and associated components of launch vehicles was applied to an existing Evolved Expendable Launch Vehicle (EELV) and the External Tank (ET) of the Space Shuttle for verification and correlation. These two vehicles were selected for validation of the methodology because extensive non-proprietary weight breakdown statements for the vehicles were available and the required information for the load cases could be determined from their trajectories. After calculating the load-bearing structural weight of the vehicle components, statistical techniques were used to estimate the relationship between the weight calculated by GT-STRESS and the actual vehicle load-bearing structural weights.

Evolved Expendable Launch Vehicle Analysis

The EELV used for verification of the methodology investigated in this study is based on the Boeing Delta-IV Heavy EELV, which is displayed in Figure 15. The launch vehicle geometry, inert masses, propellant masses, material type, and structural configuration are very similar to that of the Delta-IV Heavy. The trajectory for the EELV was modeled after the Geostationary Transfer Orbit (GTO) mission for the Delta-IV Heavy and simulated using POST. Majority of the information used to estimate the values for the vehicle parameters and trajectory came from the *International Reference Guide to Space Launch Systems*.[16] The dimensions, masses, and structure properties of the EELV are presented in Table X.

After collecting all of the required information, a GT-STRESS input file was created for the vehicle. The load conditions examined for the vehicle were liftoff, maximum dynamic pressure (max q), maximum dynamic pressure and angle of attack (max q-alpha), maximum thrust, and maximum axial acceleration. The required parameters for each load case were obtained from the simulated trajectory determined by POST and are listed in Table XI. Since GT-STRESS's modeling capability is limited to a single fuselage with all of its associated components arranged in-line throughout the length of the vehicle, the Liquid Rocket Boosters (LRBs) were modeled as point loads at their attachment location to the core booster. The LRB structure remains constant at the point for the load conditions it is involved with and the propellant loads are modeled by their percentage with each load condition. In the final load condition the LRBs are not modeled with the vehicle since they have already separated, and this load condition has an independent input file from the others since the weight statement for the input file was different from the others.

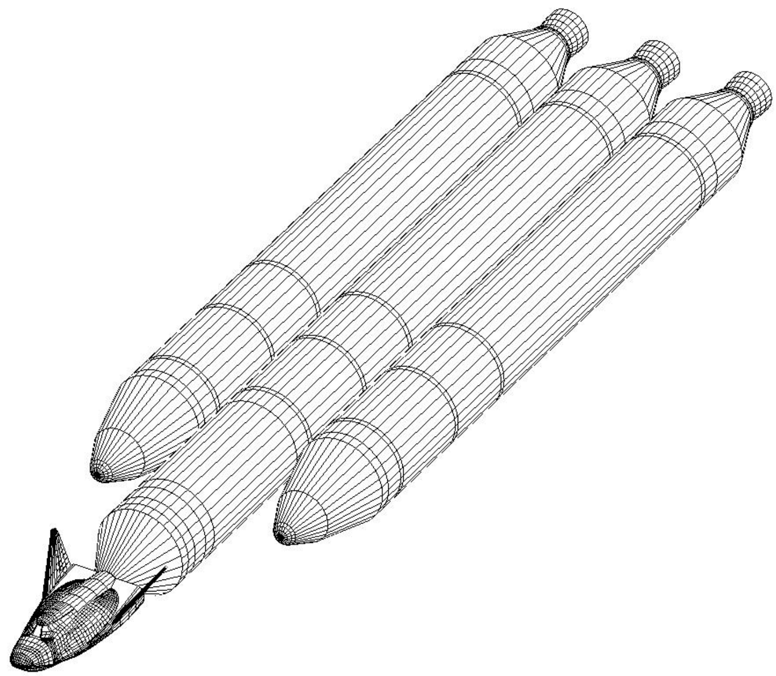

Figure 15. Boeing Delta-IV Heavy EELV

Table X. Dimensions, Masses, and Structure Properties of the EELV.[16]

	Stage 1	Stage 2
Dimensions		
Length	133.9 ft	39.9 ft
Diameter	16.7 ft	16.7 ft
Mass		
Propellant Mass	440 klb	60 klb
Inert Mass	59 klb	7.7 klb
Gross Mass	499 klb	67.7 klb
Structure		
Type	Tanks: isogrid Interstage: skin-stringer Centerbody: skin-stringer	LH_2 tank: isogrid LOX tank: monocoque
Material	Tanks: aluminum Interstage: graphite-epoxy Centerbody: graphite-epoxy	aluminum

Table XI. EELV Load Cases and Required Parameters.

Load case	1	2	3	4	5
title	liftoff	max q	max q-alpha	max thrust	max axial accel
x1 (in)	2284	0	0	0	0
x2 (in)	2285	2285	2285	2285	2285
axial_accel (g's)	1.1945	1.44	2.193	5.6162	6.0
normal_accel (g's)	6.92E-5	0.0001	0.514	0.0012	6.4E-4
prop_ullage (psi)*	30	30	30	10	10
	30	30	30	10	10
	30	30	30	10	
	30	30	30	10	
pct_ fuel (%)*	100	71	53.3	7.28	5.26
	100	71	53.3	7.28	5.26
	100	67	36	10	
	100	67	36	10	

*order of propellant tanks: CCB LOX, CCB LH_2, LRB LOX, LRB LH_2

The focus of the analysis for the EELV was the common core booster (CCB). Within the CCB the focus of the analysis is determining the structure weight of the components of the first stage since the geometry and weights for second stage and fairing are not given in detail. The structural components that are selected are the first stage liquid hydrogen tank, liquid oxygen tank, centerbody (intertank), and interstage. The propellant tanks structure type was substituted with the truss-core sandwich configuration since GT-STRESS could not accommodate the isogrid structure type. The graphite-epoxy for the interstage and centerbody were substituted with the composite material defined in the material database since the properties of that particular graphite-epoxy were unknown. Actual weights of the structural components under investigation are listed in Table XII. The input files for the EELV are located within Appendix D.

Table XII. Actual Structural Component Weights for the EELV.

Component	Weight (lb)
EELV LOX tank	4926
EELV LH2 tank	10937
EELV Centerbody	3719
EELV Interstage	5365

Space Shuttle External Tank

The entire inert mass, propellant mass, material, and geometry information for the space shuttle external tank was made available from the *Shuttle Design Data and Mass Properties* comprised by Lockheed Martin Engineering & Science Services.[17] The dimensions, masses, and structure properties of the ET are presented in Table XIII. A picture of the space shuttle external tank is presented in Figure 16.

Table XIII. Dimensions, Masses, and Structure Properties of the ET.[16]

	External Tank
Dimensions	
Length	154.2 ft
Diameter	27.6 ft
Mass	
Propellant Mass	1589 klb
Inert Mass	59.5 klb
Gross Mass	1648 klb
Structure	
Type	Skin-Stringer
Material	Aluminum

Figure 16. Space Shuttle External Tank.

("Shuttle external tank deal extended with Lockheed", Spaceflight News, June 14, 2002)

After accumulating all of the required information, a GT-STRESS input file was created for the ET. The trajectory for the Space Shuttle ascension was simulated using the POST sample input file for the Space Shuttle. Similar to the LRBs for the EELV, the Solid Rocket Boosters (SRBs) were modeled as point loads at their attachment location to the ET. Since the amount of propellant for the SRBs change at each load condition, each load condition was ran individually in GT-STRESS because the weight statement for each input file is different. The orbiter is modeled as two point loads at the locations of the orbiter attachment bars on the ET. The load conditions examined for the ET and their required parameters are presented in Table XIV.

Table XIV. ET Load Cases and Required Parameters

Load case	1	2	3	4
title	liftoff	max q	max q-alpha	max thrust
x1 (in)	1847	666	666	690
x2 (in)	1848	1372	1372	1723
axial_accel (g's)	1.2356	1.3193	1.462	2.9976
normal_accel (g's)	0	0.3857	0.3477	6.2E-6
prop_ullage (psi)*	31	31	31	30
	36	36	36	30
pct_ fuel (%)*	100	83	87	3.0
	100	83	87	3.0

*order of propellant tanks: LOX, LH_2

The focus of the analysis for the ET was determining the structural weight of the liquid hydrogen tank, the liquid oxygen tank, and the interstage. The structural components within the input file are the liquid hydrogen tank, the liquid oxygen tank, and the interstage. The input files for the external tank are located within Appendix E and the actual weights for the external tank components are in Table XV. Note that the ET Intertank weight does not include the attachment load bar for the SRBs in order to only account for the structural weight of the component.

Table XV. Actual Structural Weights for the ET.

Component	Weight (lb)
ET LOX tank	12520
ET LH2 tank	31739
ET Intertank	10374

GT-STRESS Result Data for Validation Cases

The structural component weights and total vehicle structural weight calculated by GT-STRESS for the EELV and ET are given in Table XVI. Portions of the output files generated for the EELV analysis are presented in Appendix F. Graphs of the Axial Load Magnitude along the fuselage length for each load condition of the EELV and ET are displayed in Figures 17 and 18, respectively. Graphs of the Axial Load Magnitude, Shear Load, and Bending Moment along the fuselage length for each load condition of the EELV and ET are located in Appendix G and H. A graph of the fuselage shell and frame thicknesses along the fuselage length for the EELV and ET are presented in Figure 19 and 20.

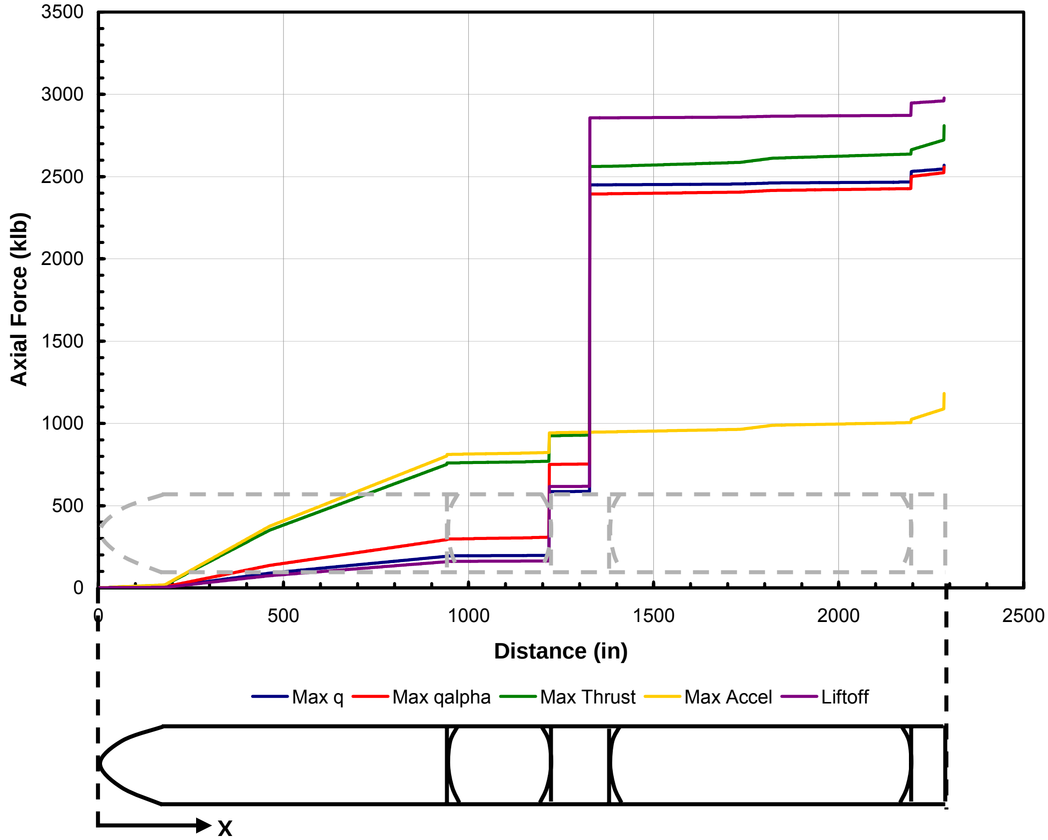

Figure 17. Axial Load Magnitude Variation along the EELV Fuselage for each Load Condition.

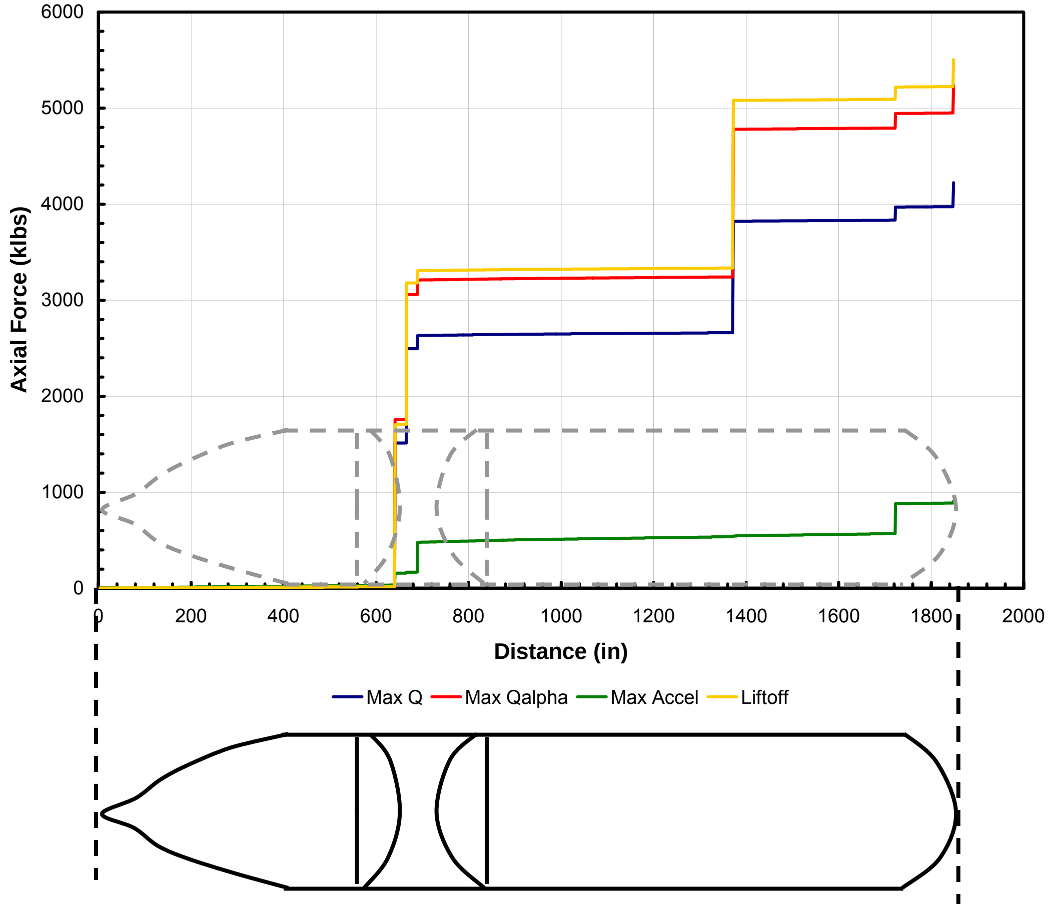

Figure 18. Axial Load Magnitude Variation along the ET for each Load Condition.

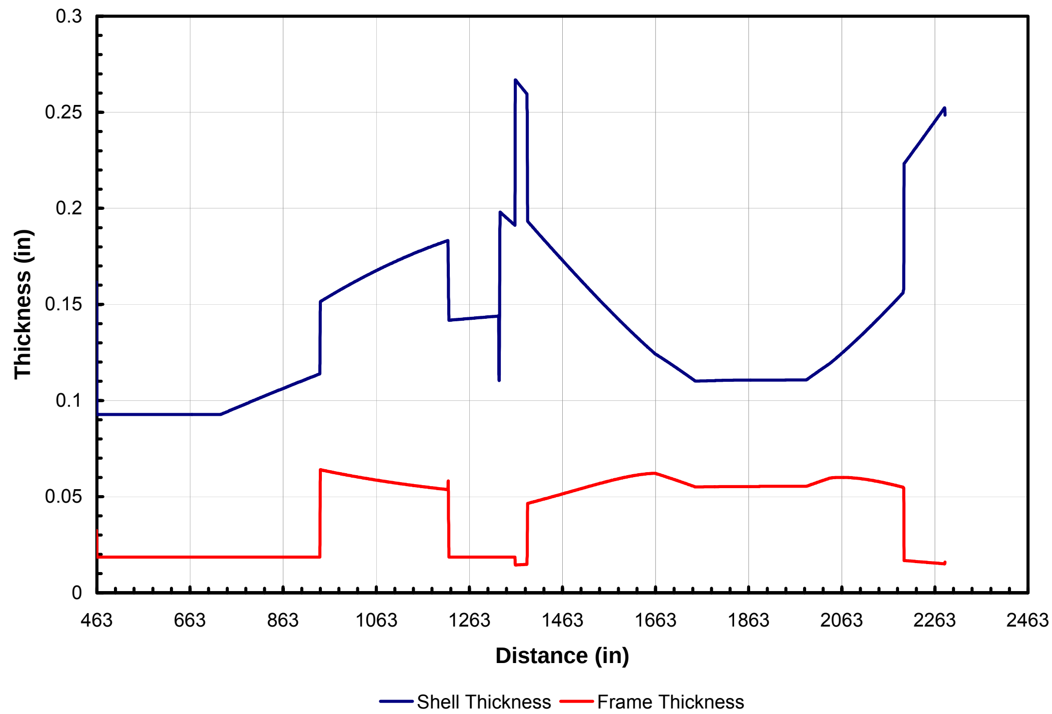

Figure 19. Fuselage Shell and Frame Thickness Variation along the EELV.

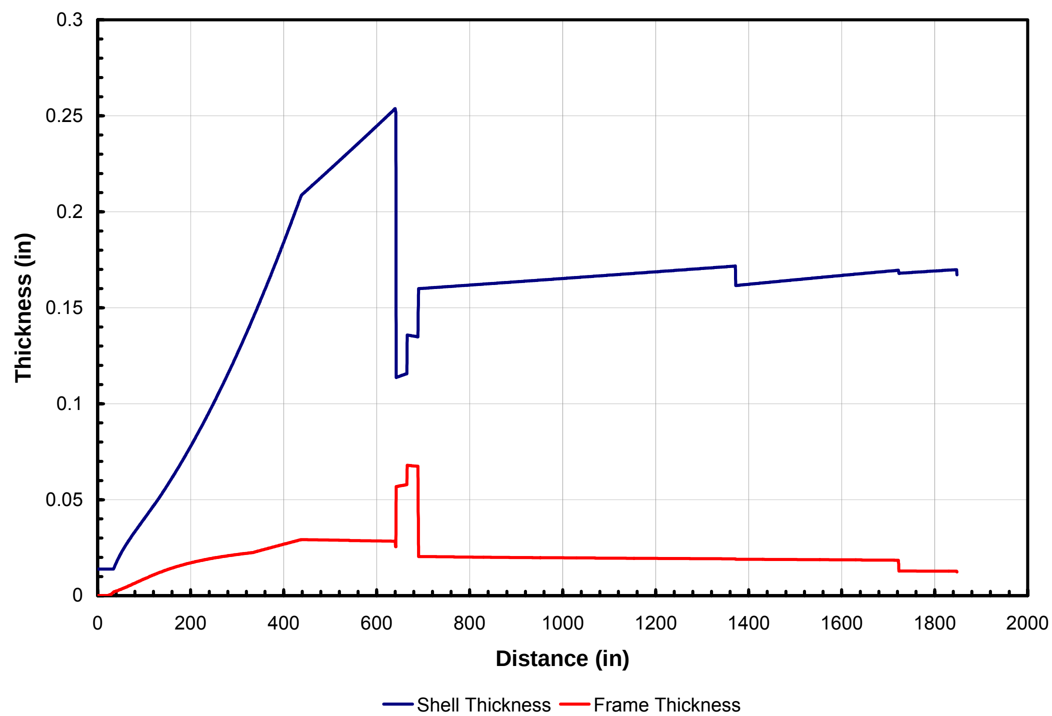

Figure 20. Shell and Frame Thickness Variation along the ET.

Table XVI. Actual and Calculated Structural Weights for the EELV and ET.

	Actual Weight (lb)	GT-STRESS Weight (lb)	% Error
ET LOX tank	12520	8970	28.35
ET LH2 tank	31739	22502	29.10
ET Intertank	10374	5662	45.42
EELV LOX tank	4926	3977	19.27
EELV LH2 tank	10937	9709	11.22
EELV Centerbody	3719	2036	38.77
EELV Interstage	5365	2277	57.56

The percent error between the actual structural component weight and the weight calculated from GT-STRESS ranges from 11.22% to 57.56%. On average, the error for the propellant tanks is significantly smaller than the error values for the other components. Regardless of the component type, the large percent error overall indicated that the structural analysis method used to estimate the fuselage stiffened shell and stability frame weight was unable to account for the total structural component weight. In order to resolve the large error, a linear regression of the actual structural weight by the calculated weight was conducted in order to determine a factor that accounts for the percentage of the structure weight not represented in the analytical method.

Regression Analysis

By determining the actual fuselage component weights from the weight statements of the two launch vehicles, a relation between the calculated load-bearing structure weights obtained from GT-STRESS and the actual load-bearing structure weights and primary structure weights are determined using linear regression. Applying linear regression develops the relation of the estimated component weights of the launch vehicle to the calculated weights from GT-STRESS using a straight line

$$y = \beta_1 x + \beta_0 \tag{53}$$

where y is the value of the estimated weight, β_1 is the slope of the regression line, x is the weight value obtained from GT-STRESS, and β_0 is the y-intercept. The regression line is determined by using the *method of least squares*, where the sum of the squares of the residual errors between the actual data points and the estimated data points on the regression line is minimized. Therefore a straight line is drawn through the ordered pairs of weight data so that the collective deviation of the actual weight above or below the line is minimized. Using the regression technique allows for the formation of an expression for the estimated weight as a function of the calculated weight from GT-STRESS.

The accuracy of the regression in the prediction of the estimated component structural weight from the GT-STRESS calculated weight is represented by the coefficient of variation, which is also denoted as the R^2 value. The R^2 value is interpreted as the reduction in residual error due to the regression technique.[1] An R^2 value of 1 represents a perfect fit of the regression line to the data while an R^2 value of zero represents denotes that regression analysis does not provide any improvement in fitting the data. The regression analysis and determination of the R^2 value for the structural weight data used with this study was conducted using Microsoft EXCEL.

The regression analysis previously described is used to develop a relationship between the component structural weights calculated from GT-STRESS and the actual component weights. For the regression line the y-intercept term is set to zero knowing that a calculated weight of zero will result in a true actual weight of zero. This simplified version of the linear equation allows the expression to be applied to a large spread of weights and compared with other regression data for analytical weight estimation.

The analytical methodology implemented into the GT-STRESS program only predicts the load-bearing structure of the shell and stability frames. Structural weight of the components consists of all load-carrying members, which include such things as bulkheads, frames, minor frames, covering, and covering stiffeners. This classification of the structural weight is equivalent to the structural members that comprise the structures of the integral propellant tanks. Applying linear regression to the actual and calculated values of the propellant tanks of the launch vehicles used for verification yields the following equation for estimating structural weight:

$$W_{actual} = 1.3665 W_{STRESS} \tag{54}$$

The R^2 value for this linear curve-fit is 0.9948. Based on the linear regression, the calculated weight must be increased by about 36.7% to get the actual structure weight. The linear regression of the structural weight is displayed in Figure 21.

Primary weight is comprised of all load-bearing members as described for the structural weight along with supplementary structure items that are used to support the load-bearing members and secure other vehicle components to the structure. Some of these additional structure items include joints, fasteners, keel beam, fail-safe straps, attachment fittings, and pressure web.[1] This classification of the primary weight is equivalent to the structural members and secondary items that comprise the non propellant tank structures, such as the interstage, intertank, and centerbody. The resulting linear regression equation for the estimation of the primary weight from the calculated weight is

$$W_{actual} = 1.8973 W_{STRESS} \tag{55}$$

The R^2 value for this linear curve-fit is 0.9917. Based on the linear regression, the calculated weight must be increased by about 90% to get the actual primary weight. The linear regression of the primary weight is displayed in Figure 22.

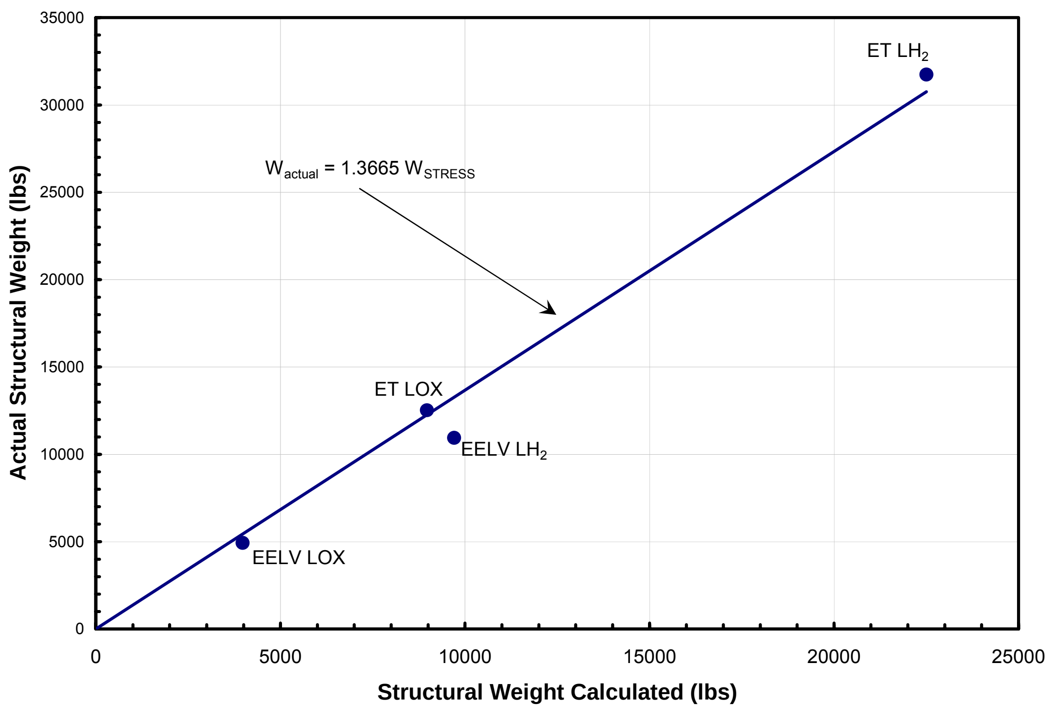

Figure 21. Linear Regression of Structural Weight.

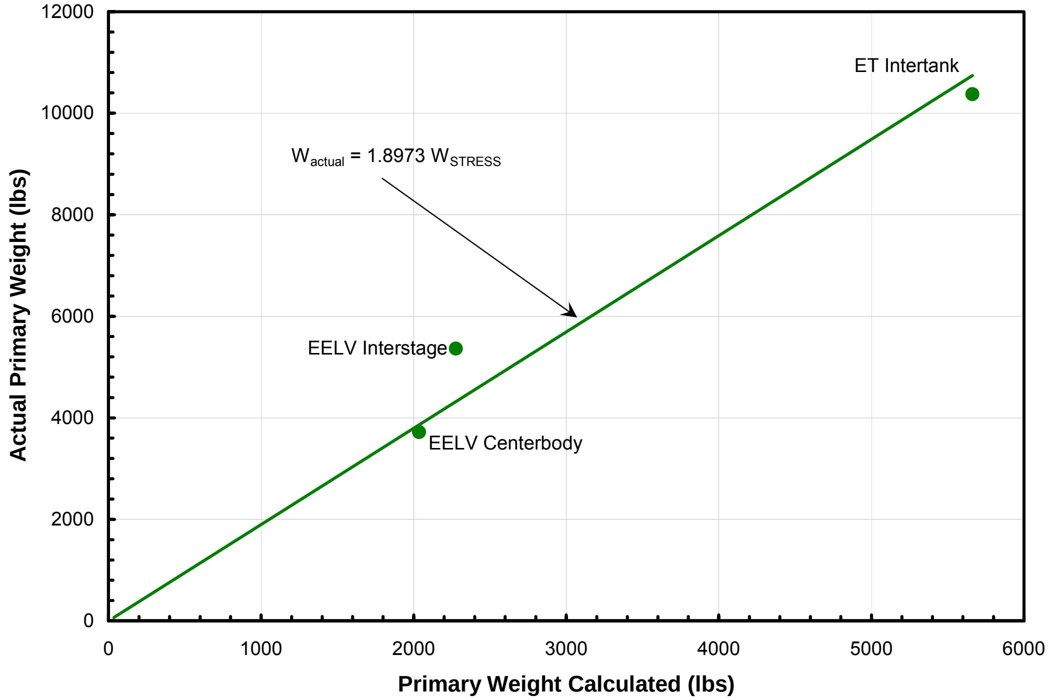

Figure 22. Linear Regression of Primary Weight.

Due to the limited quantity of data points for the regression analysis of the structural and primary weight, the resulting equations relating the component weight calculated in GT-STRESS to the actual structural and primary weights are questionable. Validation of the resulting correlation between the calculated and actual component structure weight required either a larger quantity of data points to generate a regression or that the current regression followed a trend of a larger data set that conducted a very similar analysis. In *Analytical Fuselage and Wing Weight Estimation of Transport Aircraft*, Mark Ardema and company created a computer program, PDCYL, which employed the same basic fundamental beam structure analysis used within GT-STRESS to determine the structural weight of eight conventional transport aircraft fuselage.[1] Linear regression analysis of the program generated data and the actual values yielded the following correlation for the fuselage structure and primary weights:

$$W_{actual} = 1.3503 W_{PDCYL} \tag{56}$$

$$W_{actual} = 1.8872 W_{PDCYL} \tag{57}$$

The correlations between the actual and calculated structure weights from the regression of the aircraft fuselage data are very similar to the regression equations for the launch vehicle fuselage data. The trends from the regression of the structure and primary weights for both data sets are very comparable, as displayed in Figures 23 and 24, respectively. Therefore the close resemblance of the trends and correlation of the estimated structural and primary weight from GT-STRESS to PDCYL validates that the launch vehicle fuselage and component structural weight are accurately represented.

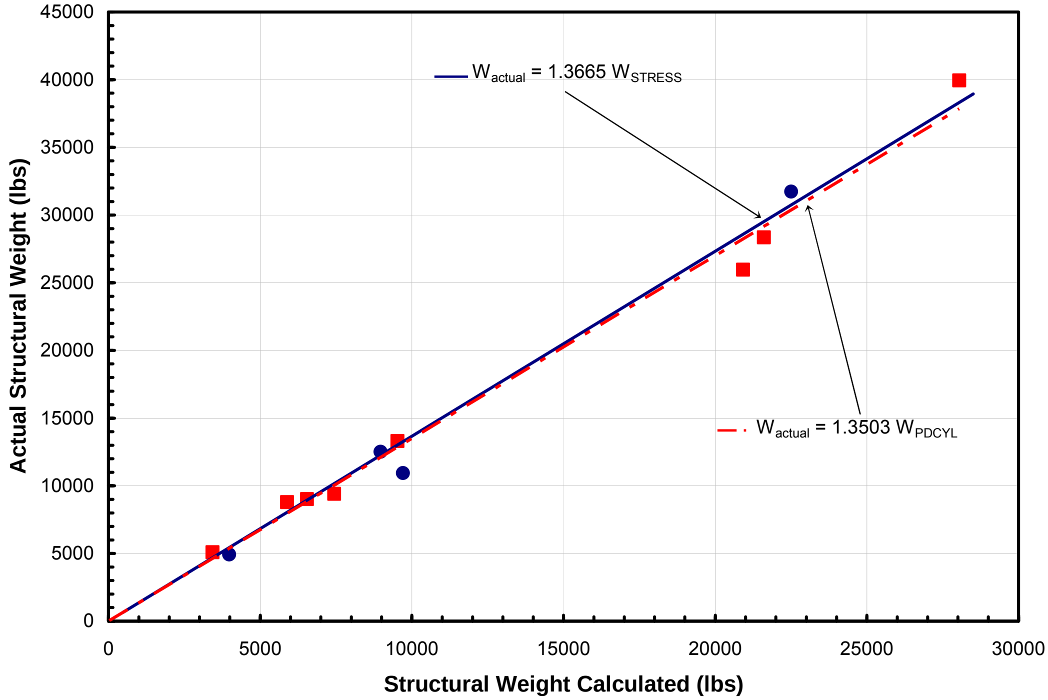

Figure 23. Regression Comparison of Structural Weight Results from GT-STRESS and PDCYL.

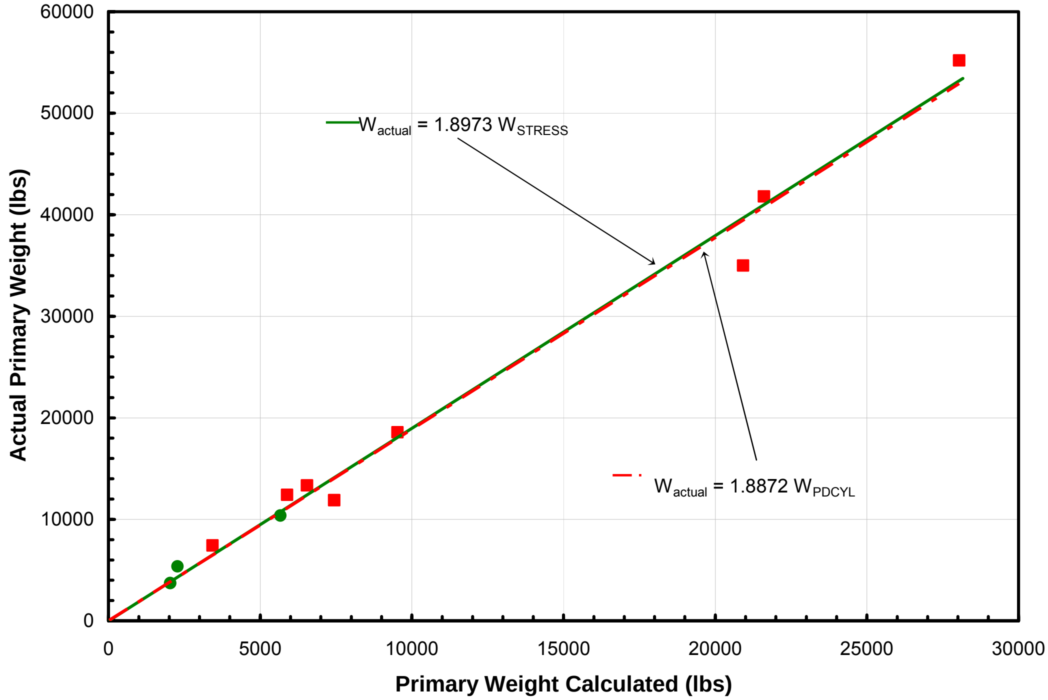

Figure 24. Regression Comparison of Primary Weight Results from GT-STRESS and PDCYL.

Integration of GT-STRESS into Multidisciplinary Environment

In addition to its functionality as a *stand alone* executable program to calculate vehicle structural weight, GT-STRESS can also be employed as another contributing analysis (CA) in the vehicle development design structure matrix. By obtaining the load condition information from the trajectory CA and the preliminary vehicle weights from the weights & sizing (W&S) CA, GT-STRESS can determine the fuselage component structural weight and primary weight. The weight breakdown of this information can be fed back to the W&S CA, and the cycle between the trajectory, W&S, and GT-STRESS CAs can continue iteration until convergence.

To demonstrate the program's ability as a CA within the design process, GT-STRESS was implemented into a multidisciplinary runtime environment program known as ModelCenter.[22] A ModelCenter Filewrapper was developed for the program which allowed the generation of an input file, execution of the program, and generation of the output data within the ModelCenter environment without any external execution. The objective of this demonstration is to determine the weight of the EELV using the multidisciplinary approach for a single iteration, verify the resulting structural weights with the values generated from the stand alone GT-STRESS, and generate a weight breakdown statement (WBS) of the vehicle using the calculated weight and the regression equations. The trajectory CA is a Microsoft EXCEL spreadsheet that delivers the acceleration and percent of remaining propellant for each load condition from the POST output for the vehicle to the GT-STRESS CA. The GT-STRESS CA calculates the component structure weight using the delivered load condition information and the previously defined information from the input file, and transfers the calculated component weights to the W&S CA. The W&S CA is also a spreadsheet that multiplies the weights by their associated correlation factors and determines the entire structure weight breakdown of the vehicle. A design structure matrix (DSM) of the information process between the CA's is presented in Figure 25.

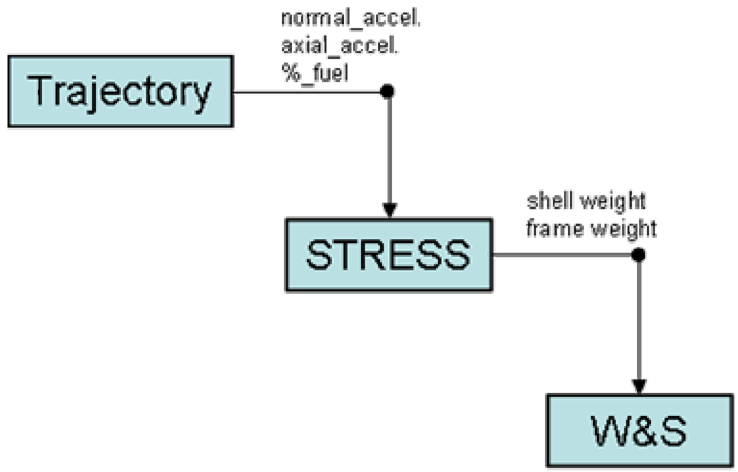

Figure 25. Design Structure Matrix.

As expected, the calculated values of the structure weight from the GT-STRESS CA were the same as the values calculated from the stand alone version, proving that the data flow of load condition information from the trajectory CA was successful. The W&S CA generated a WBS for the EELV structure weight based on the product of the weights transferred from the GT-STRESS CA and their corresponding correlation factors. Printed copies of the spreadsheets for the trajectory CA and W&S CA are located in Appendix I. A view of the ModelCenter interface with the three CAs and the resulting weight values is displayed in Figure 26. The actual component structure weight values, the GT-STRESS calculated values, and the GT-STRESS-correlated weight values are presented in Table VIII.

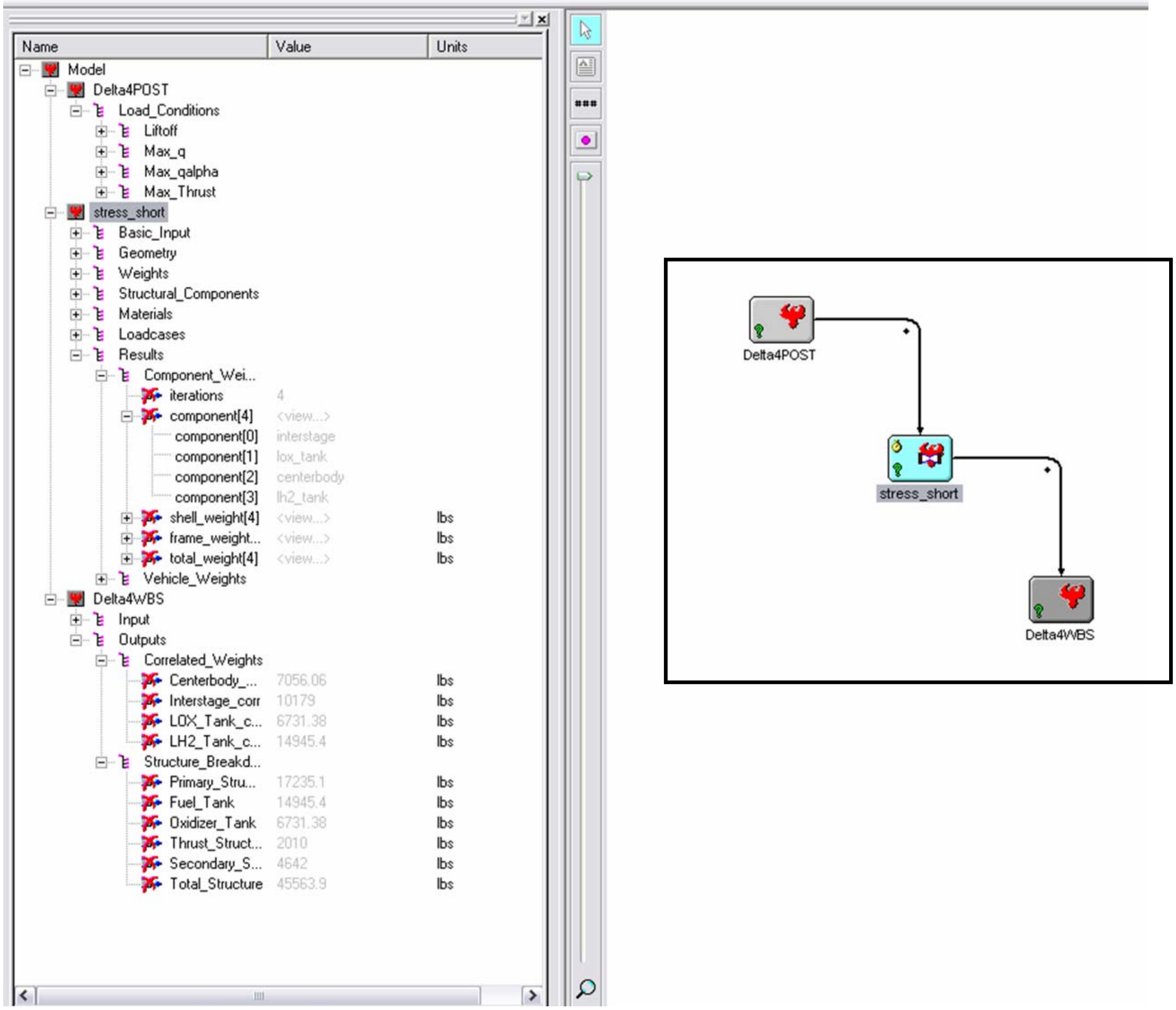

Figure 26. ModelCenter Interface of Multidisciplinary Analysis Demonstration.

Table XVII. Actual and Correlated Structural Weights for the EELV and ET.

	Actual Weight (lb)	GT-STRESS Weight (lb)	% Error
ET LOX tank	12520	12257	2.10
ET LH2 tank	31739	30749	3.12
ET Intertank	10374	10742	3.55
EELV LOX tank	4926	5436	10.35
EELV LH2 tank	10937	13268	21.31
EELV Centerbody	3719	3863	3.87
EELV Interstage	5365	4320	19.48

Conclusion

A method based on fundamental beam structure analysis to accurately determine structural weight of the vehicle fuselage and components at a minimized cost of time and computational effort was developed. The analytical methodology was implemented into the software tool GT-STRESS for rapid estimation of fuselage & component load-bearing structural weight. The correlation and accuracy of calculating structural component weight by GT-STRESS was verified by sizing components of existing launch vehicles and comparing the results to a similar methodology employed for transport aircraft fuselage weight estimation.

Acknowledgements

The author would like to thank Jeff Cerro at NASA Langley Research Center and the members of the Space Systems Design Lab (SSDL) at Georgia Institute of Technology for their assistance and support during the development of this project.

References

1. Ardema, M.D., et. al, *Analytical Fuselage and Wing Weight Estimation of Transport Aircraft*. NASA/TM-110392, May 1996.
2. Crawford, R.F., Burns, A.B., *Minimum Weight Potentials for Stiffened Plates and Shells*. AIAA Journal, April 1963; Vol. 1: No. 4.
3. *Circumference/Perimeter of an Ellipse.* Numericana. Available from: http://home.att.net/~numericana/answer/ellipse.htm
4. Cerro, J.A., *RL, a Computer Program to Calculate Running Loads for Integral-Tank Aerospace Vehicle Fuselages*. Hampton, VA: Lockheed Martin Engineering & Science Services, April 1996.
5. Jawad, M.H., *Design of Plate & Shell Structures*. New York: American Society of Mechanical Engineers, 2004.
6. Powell, R.W., et. al., *Program To Optimize Simulated Trajectories (POST), Utilization Manual, Volume II, Version 5.2.* Hampton, VA: NASA Langley Research Center, Denver, CO: Martin Marietta Corporation, October 1997
7. Beer, F.P. and Johnston, E.R., *Vector Mechanics for Engineers: Statics*. Sixth Edition. New York: McGraw-Hill, 1996.
8. Hibbler, R.C., *Mechanics of Materials*. Fourth Edition. Upper Saddle River, NJ: Prentice Hall, 2000.
9. Shigley, J.E., *Mechanical Engineering Design*. Second Edition. New York: McGraw-Hill, 1972.
10. Bauchau, O.A., *Aerospace Structural Analysis*. Atlanta, GA: Georgia Institute of Technology, December 2002.
11. *Fundamentals of Lightweight Design: Formulary*. Institute for Lightweight Construction, Rheinisch-Westfaeli Technical University Aachen. Available from: http://www.ilb.rwth-aachen.de/KLAUSUREN/formel.pdf
12. Brun, E.F., *Analysis and Design of Flight Vehicle Structures*. Fourth Edition. Cincinnati, OH: Tri-State Offset, 1965.
13. *Ellipse*. Wolfram Research. Available from: http://mathworld.wolfram.com/Ellipse.html
14. Shanley, F.R., *Weight Strength Analysis of Aircraft Structures.* Second Edition. New York: Dover Press, 1960.
15. Crawford, R.F., Burns, A.B., *Minimum Weight Potentials for Stiffened Plates and Shells*. AIAA Journal, April 1963; Vol. 1: No. 4.
16. Isakowitz, S.J., et. al., *International Reference Guide to Space Launch Systems*. Third Edition. Reston, VA: AIAA, 1999.
17. MacConochie, I.O., *Shuttle Design Data and Mass Properties*. Hampton, VA: Lockheed Martin Engineering & Science Services, April 1992.
18. Sutton, G.P., *Rocket Propulsion Elements: An Introduction to the Engineering of Rockets*. Sixth Edition. New York: John Wiley & Sons, 1992.
19. Bai, S.D., Dumbacher, P., Cole, J.W., *Development of Advanced Hydrocarbon Fuels at Marshall Space Flight Center*. NASA/TP-2002-211729
20. Wertz, J.R. and Larson, W.J., *Space Mission Analysis and Design*. Third Edition. Torrance, CA: Microcosm Press, 1999.
21. "Shuttle external tank deal extended with Lockheed", NASA News Release, Spaceflight Now. June 14, 2002. Available from: http://spaceflightnow.com/news/n0206/17tank/

22. ModelCenter 5.0.1. Blacksburg, VA: Phoenix Integration, Inc., July 2003.
23. Young, D.F., Munson, B.R., Okiishi, T.H., *A Brief Introduction to Fluid Mechanics*. Second Edition. New York: John Wiley & Sons, 2001.

Appendix A: Example GT-STRESS Input file

```
Test Case for integral tank program
oal 2000
geom
  0     1     1
  160   85    85
  600   200   200
  1800  200   200
  2000  100   100
end_geom
weights
  wing              1440 2000 10000
  fwd_gear  160 160 1000
  aft_gear  1440 1440 7000
  lox_tank  150 690 8000
  lh2_tank  1180 1840 12000
  nose              0 175 2025
  intertank 690 1180 15000
  thrust_str      1790 2000 3000
  tps         0 2000 20000
  misc          0 2000 5000
  main_engines    2000 2000 50000
  plumbing  0 2000 10000
  fwd_rcs_oms     90 90 1000
  aft_rcs_oms     2000 2000 2000
  avionics  90 90 2000
  payload   750 1140 25000
  propellant    150 690 2000000   lox
  propellant    1180 1840 200000  lox
end_weights
structure
  lox_tank
  lh2_tank
  intertank
end_structure
material
  default_shell z-stiffened
  default_mat   aluminum
  aluminum      180 200   z-stiffened
  other         250 300   z-stiffened
  beryllium     501 1000  z-stiffened
  titanium      1080 2000 z-stiffened
end_material
loadcase 1
  title           Liftoff
  x1                    160
  x2                    1440
  axial_accel           1.32
  normal_accel          0.5
  prop_ullage           25 25
  pct_fueled            100 100
end_loadcase
loadcase 2
  title           Max q-alpha
  x1                    1440
  x2                    2000
```

```
  axial_accel           1.88
  normal_accel          0.5
  prop_ullage           25 25
  pct_fueled            72 72
end_loadcase
loadcase 3
  title           Subsonic Pullup
  x1                    1440
  x2                    2000
  axial_accel           0
  normal_accel          2.5
  prop_ullage           25 25
  pct_fueled              0 0
end_loadcase
loadcase 4
  title           2.0G Main Gear Landing
  x1                    1440
  x2                    1450
  axial_accel           0
  normal_accel          2.0
  prop_ullage           10 10
  pct_fueled              0 0
end_loadcase
loadcase 5
  title                 2.0 G All gear landing
  x1                    160
  x2                    1440
  axial_accel           0
  normal_accel          2.0
  prop_ullage           10 10
  pct_fueled            0 0
end_loadcase
```

Appendix B: Default Propellant Text File (propellant.txt)

Propellant	Density(lb/ft^3)	Description
lox	71.293	Liquid Oxygen
LOX	71.293	Liquid Oxygen
lh2	4.432	Liquid Hydrogen
LH2	4.432	Liquid Hydrogen
h2o2	88.2732	Hydrogen Peroxide
H2O2	88.2732	Hydrogen Peroxide
n2o4	89.8963	Nitrogen Textroxide
N2O4	89.8963	Nitrogen Textroxide
rp1	50.5667	Rocket Fuel
RP1	50.5667	Rocket Fuel
RP-1	50.5667	Rocket Fuel
n2h4	63.0523	Hydrazine
N2H4	63.0523	Hydrazine
mmh	54.8118	Monomethyl Hydrazine
MMH	54.8118	Monomethyl Hydrazine
udmh	49.2557	Unsymmetrical Dimethyl Hydrazine
UDMH	49.2557	Unsymmetrical Dimethyl Hydrazine
fl	94.2038	Liquid Flourine
Fl	94.2038	Liquid Flourine
FL	94.2038	Liquid Flourine
f2	94.2038	Liquid Flourine
F2	94.2038	Liquid Flourine
ch4	27.7804	Methane
CH4	27.7804	Methane
methane	27.7804	Methane
METHANE	27.7804	Methane
jp	48.6938	Jet Fuel
JP	48.6938	Jet Fuel
quad	61.0982	Quadricyclane(C7H8) - MSFC Hydrocarbon
QUAD	61.0982	Quadricyclane(C7H8) - MSFC Hydrocarbon
bcp	52.7766	BCP(C6H8) - Hydrocarbon Fuel from MSFC
BCP	52.7766	BCP(C6H8) - Hydrocarbon Fuel from MSFC
afrl1	48.7001	AFRL-1 - Hydrocarbon Fuel from AFRL
AFRL1	48.7001	AFRL-1 - Hydrocarbon Fuel from AFRL
AFRL-1	48.7001	AFRL-1 - Hydrocarbon Fuel from AFRL
cinch	58.1017	CINCH(C4H10N4) - Hydrocarbon from MSFC
CINCH	58.1017	CINCH(C4H10N4) - Hydrocarbon from MSFC
octad	51.0036	Octadiyne(C8H10) - Hydrocarbon from MSFC
OCTAD	51.0036	Octadiyne(C8H10) - Hydrocarbon from MSFC

<u>Appendix C: Default Material Text File (material.txt)</u>

```
Material     E(psi)      rho(lb/in^3)     UTS(psi)    YS(psi)     min gauge(in)    Notes
aluminum     10300000    0.101            67000       55000       0.0056
titanium     16000000    0.160            130000      124000      0.0075
beryllium    43900000    0.0666           53700       34800       0.0056
magnesium    6500000     0.064            39000       24000       0.0056
steel        29700000    0.284            108000      68200       0.0075           airframe/rocket casing
composite    27557171    0.065029         117481      76870       0.0375           Aerospace Composite…
al-li        11200000    0.0918           74000       65300       0.0056           Aluminum-Lithium Alloy
other        15600000    0.178            66000       65000       0.0056           Just used for testing…
composite2   10200000    0.065029         117481      76870       0.0375           Aerospace Grade Carbon
Fiber Epoxy Composite
```

Appendix D: Input Files for the EELV Verification Case

Input File #1

```
EELV (with LRBs)
oal 2285
geom
  0     1      1
  20    18     18
  198   100    100
  2285  100    100
end_geom
weights
  fairing       0     462   7860
  interstage    463   942   5365
  lox_tank      943   1218  4926
  strap_ons     1328  1328  114602
  centerbody    1157  1387  3719
  lh2_tank      1388  2196  10937
  thrust_str      2197  2285  10492
  main_engine   2285  2285  15394
  aft_skirt     1734  1822  3488
  tunnel_assem  942   942   1439
  assem_prod1   363   2285  680
  prop_prod     463   2285  2010
  assem_prod2   0     2285  279
  2nd_stage     463   942   68662
  payload   180   462   54282
  propellant    943   1218  377143  lox
  propellant    1388  2196  62857   lh2
  propellant    1327  1328  754286  lox
  propellant    1327  1328  125715  lh2
end_weights
structure
  lox_tank
  lh2_tank
  centerbody
  interstage
end_structure
material
  default_shell z-stiffened
  default_mat   aluminum
  aluminum      943   1218   sandwich
  aluminum      1388  2196   sandwich
  composite     463   942    z-stiffened
  composite     1219  1361   z-stiffened
  composite     0     462    sandwich
end_material
loadcase 1
  title           Liftoff
  x1                    2284
  x2                    2285
  axial_accel                 1.1945
  normal_accel          0.0000692
  prop_ullage           30. 30. 30 30
  pct_fueled              100. 100. 100 100
end_loadcase
```

```
loadcase 2
  title           Max q
  x1                    0
  x2                    2285
  axial_accel                 1.44
  normal_accel          0.0001
  prop_ullage           30. 30. 30. 30.
  pct_fueled              71 71 67 67
end_loadcase
loadcase 3
  title           Max q-alpha
  x1                    0
  x2                    2285
  axial_accel                 2.193
  normal_accel          0.514
  prop_ullage           30 30 30. 30.
  pct_fueled              53.3 53.3  36 36
end_loadcase
loadcase 4
  title           Max Thrust
  x1                    0
  x2                    2285
  axial_accel                 5.6162
  normal_accel          0.0012
  prop_ullage           10. 10. 10 10
  pct_fueled              7.28 7.28 10 10
end_loadcase
```

Input File #2

```
EELV (without LRBs)
oal 2285
geom
  0     1      1
  20    18     18
  198   100    100
  2285  100    100
end_geom
weights
  fairing       0     462   7860
  interstage    463   942   5365
  lox_tank      943   1218  4926
  centerbody    1157  1387  3719
  lh2_tank      1388  2196  10937
  thrust_str      2197  2285  10492
  main_engine   2285  2285  15394
  aft_skirt     1734  1822  3488
  tunnel_assem  942   942   1439
  assem_prod1   363   2285  680
  prop_prod     463   2285  2010
  assem_prod2   0     2285  279
  2nd_stage     463   942   68662
  payload   180   462   54282
  propellant    943   1218  377143  lox
  propellant    1388  2196  62857   lh2
end_weights
structure
  lox_tank
  lh2_tank
  centerbody
  interstage
end_structure
material
  default_shell z-stiffened
  default_mat   aluminum
  aluminum      943   1218  sandwich
  aluminum      1388  2196  sandwich
  composite     463   942   z-stiffened
  composite     1219  1361  z-stiffened
  composite     0     462   sandwich
end_material
loadcase 1
  title                 Max Axial Acceleration
  x1                0
  x2                    2285
  axial_accel                6
  normal_accel          0.00064
  prop_ullage           10. 10.
  pct_fueled              5.26 5.26
end_loadcase
```

Appendix E: Input Files for the External Tank Verification Case

Input File #1

```
External Tank of Shuttle (with RSRMs at 100%)
oal 1848
geom
  0     1       1
  438   165.6   165.6
  1848  165.6   165.6
end_geom
weights
  lox_tank      0     641   12520
  propellant    24    641   1362000 lox
  intertank     626   911   13480
  lh2_tank      690   1848  31739
  propellant    690   1848  227000  lh2
  RSRM_1        666   666   1190756
  RSRM_2        1372  1372  1409324
  tps           0     1848  7128
  prop_mech     0     1848  3755
  electrical    626   911   598
  srb_attach1   666   666   2744
  srb_attach2   1372  1372  2744
  range_safety  626   911   396
  mfg_var_wgt   0     1848  708
  unused_liq    0     1848  391
  gases         0     1848  3948
  sep_hardware1 666   666   441
  sep_hardware2 1372  1372  442
  orbiter_1     690   690   103500
  orbiter_2     1723  1723  103500
end_weights
structure
  lox_tank
  lh2_tank
  intertank
end_structure
material
  default_shell z-stiffened
  default_mat   aluminum
end_material
loadcase 1
  title           Liftoff
  x1                    1847
  x2                    1848
  axial_accel           1.2356
  normal_accel          0
  prop_ullage           31   36
  pct_fueled            100  100
end_loadcase
```

Input File #2

```
External Tank of Shuttle (with RSRMs at 55%)
oal 1848
geom
  0     1       1
  438   165.6   165.6
  1848  165.6   165.6
end_geom
weights
  lox_tank      0     641   12520
  propellant    24    641   1362000 lox
  intertank     626   911   13480
  lh2_tank      690   1848  31739
  propellant    690   1848  227000  lh2
  RSRM_1        666   666   740502
  RSRM_2        1372  1372  876386
  tps           0     1848  7128
  prop_mech     0     1848  3755
  electrical    626   911   598
  srb_attach1   666   666   2744
  srb_attach2   1372  1372  2744
  range_safety  626   911   396
  mfg_var_wgt   0     1848  708
  unused_liq    0     1848  391
  gases         0     1848  3948
  sep_hardware1 666   666   441
  sep_hardware2 1372  1372  442
  orbiter_1     690   690   103500
  orbiter_2     1723  1723  103500
end_weights
structure
  lox_tank
  lh2_tank
  intertank
end_structure
material
  default_shell z-stiffened
  default_mat   aluminum
end_material
loadcase 1
  title           Max Dynamic Pressure
  x1                    666
  x2                    1372
  axial_accel           1.3193
  normal_accel          0.3857
  prop_ullage           31   36
  pct_fueled            83   83
end_loadcase
```

Input File #3

```
External Tank of Shuttle (with RSRMs at 66.67%)
oal 1848
geom
  0     1       1
  438   165.6   165.6
  1848  165.6   165.6
end_geom
weights
  lox_tank      0     641   12520
  propellant    24    641   1362000 lox
  intertank     626   911   13480
  lh2_tank      690   1848  31739
  propellant    690   1848  227000  lh2
  RSRM_1        666   666   886044
  RSRM_2        1372  1372  1048622
  tps           0     1848  7128
  prop_mech     0     1848  3755
  electrical    626   911   598
  srb_attach1   666   666   2744
  srb_attach2   1372  1372  2744
  range_safety  626   911   396
  mfg_var_wgt   0     1848  708
  unused_liq    0     1848  391
  gases         0     1848  3948
  sep_hardware1 666   666   441
  sep_hardware2 1372  1372  442
  orbiter_1     690   690   103500
  orbiter_2     1723  1723  103500
end_weights
structure
  lox_tank
  lh2_tank
  intertank
end_structure
material
  default_shell z-stiffened
  default_mat   aluminum
end_material
loadcase 1
  title           Max Q-alpha
  x1                  666
  x2                  1372
  axial_accel         1.462
  normal_accel        0.3477
  prop_ullage         31   36
  pct_fueled          87   87
end_loadcase
```

Input File #4

```
External Tank of Shuttle (without RSRMs)
oal 1848
geom
  0     1       1
  438   165.6   165.6
  1848  165.6   165.6
end_geom
weights
  lox_tank      0     641   12520
  propellant    24    641   1362000 lox
  intertank     626   911   13480
  lh2_tank      690   1848  31739
  propellant    690   1848  227000  lh2
  tps           0     1848  7128
  prop_mech     0     1848  3755
  electrical    626   911   598
  srb_attach1   666   666   2744
  srb_attach2   1372  1372  2744
  range_safety  626   911   396
  mfg_var_wgt   0     1848  708
  unused_liq    0     1848  391
  gases         0     1848  3948
  orbiter_1     690   690   103500
  orbiter_2     1723  1723  103500
end_weights
structure
  lox_tank
  lh2_tank
  intertank
end_structure
material
  default_shell z-stiffened
  default_mat   aluminum
end_material
loadcase 1
  title           Max Axial Acceleration
  x1                    690
  x2                    1723
  axial_accel           2.9976
  normal_accel          0.0000062
  prop_ullage           30   30
  pct_fueled            3    3
end_loadcase
```

Appendix F: Output Files Generated for the EELV Verification Case

EELV.cog

```
- Center of Gravity File -

Center of Gravity for Iteration 0
Center of gravity for loadcase 1: 1238.6 inches
Center of gravity for loadcase 2: 1223.17 inches
Center of gravity for loadcase 3: 1193.64 inches
Center of gravity for loadcase 4: 1126.92 inches
-------------------------------------------------------------------

Center of Gravity for Iteration 1
Center of gravity for loadcase 1: 1239.34 inches
Center of gravity for loadcase 2: 1224.08 inches
Center of gravity for loadcase 3: 1194.69 inches
Center of gravity for loadcase 4: 1127.97 inches
-------------------------------------------------------------------

Center of Gravity for Iteration 2
Center of gravity for loadcase 1: 1239.33 inches
Center of gravity for loadcase 2: 1224.07 inches
Center of gravity for loadcase 3: 1194.66 inches
Center of gravity for loadcase 4: 1127.91 inches
-------------------------------------------------------------------

Center of Gravity for Iteration 3
Center of gravity for loadcase 1: 1239.33 inches
Center of gravity for loadcase 2: 1224.07 inches
Center of gravity for loadcase 3: 1194.66 inches
Center of gravity for loadcase 4: 1127.91 inches
-------------------------------------------------------------------

Center of Gravity for Iteration 4
Center of gravity for loadcase 1: 1239.33 inches
Center of gravity for loadcase 2: 1224.07 inches
Center of gravity for loadcase 3: 1194.66 inches
Center of gravity for loadcase 4: 1127.91 inches
-------------------------------------------------------------------
```

EELV.dat

```
Simple Output File for EELV Heavy (with LRBs)

Component       Iter    Shell Wt(lbs)       Frame Wt(lbs)       Total Wt(lbs)
interstage      4       1913.69946289       178.781967163       2092.47998047
lox_tank        4       2957.35180664       1020.36401367       3977.71435547
centerbody      4       2047.62902832       280.793334961         2328.421875
lh2_tank        4       6814.54980469       2894.81567383       9709.37109375

                  Total vehicle shell weight:              16829.6621094 lbs
                  Total vehicle frame weight:              4261.82080078 lbs
                  Total vehicle structural weight:         21091.4824219 lbs
------------------------------------------------------------------------------
```

EELV.lod

Load File for EELV Heavy (with LRBs)

Axial Force, Shear Force, Bending Moment and Running Loads vs. Fuselage Length: Loadcase 1

X(in)	Axial(lb)	Shear(lb)	Bending(lb-in)	Nx_total(lb/in)	Ny_total(lb/in)	Nxy_total(lb/in)
0	-20.46786118	0.001185748028	0.001185748028	-4.886907578	0	0.0005661529722
1	-40.93572235	0.002371496055	0.003557244083	-5.283027649	0	0.0006120572216
2	-61.40358353	0.003557244083	0.007114488166	-5.42973423	0	0.0006290588062
3	-81.8714447	0.004742992111	0.01185747981	-5.506186008	0	0.0006379188271
4	-102.3393097	0.005928739905	0.01778621972	-5.553099632	0	0.0006433555973
5	-122.8071747	0.0071144877	0.02490070835	-5.584822178	0	0.0006470318767
6	-143.2750397	0.008300235495	0.03320094198	-5.607703209	0	0.0006496836431
7	-163.7429047	0.00948598329	0.04268692434	-5.624988556	0	0.0006516868016
8	-184.2107697	0.01067173108	0.05335865542	-5.638505936	0	0.0006532533444
9	-204.6786346	0.01185747888	0.06521613151	-5.649366379	0	0.0006545119686
10	-225.1464996	0.01304322667	0.07825935632	-5.658284187	0	0.0006555454456
11	-245.6143646	0.01422897447	0.09248833358	-5.665736675	0	0.0006564090727
12	-266.0822144	0.01541472226	0.1079030558	-5.672057152	0	0.0006571417325
13	-286.5500793	0.01660047099	0.1245035231	-5.677487373	0	0.0006577710155
14	-307.0179443	0.01778621972	0.1422897428	-5.682201385	0	0.0006583173526
15	-327.4858093	0.01897196844	0.1612617075	-5.686332703	0	0.0006587961689
16	-347.9536743	0.02015771717	0.1814194322	-5.689982414	0	0.0006592192221
17	-368.4215393	0.02134346589	0.2027629018	-5.693231583	0	0.0006595957093
18	-388.8894043	0.02252921462	0.2252921164	-5.696140766	0	0.0006599329063
19	-409.3572693	0.02371496335	0.249007076	-5.698762894	0	0.0006602367503
20	-429.8251343	0.02490071207	0.2739077806	-5.701136589	0	0.0006605118979
....						
2284	-2754531.5	334.9691772	102111.7188	-6580.834961	0	1.599359989
2285	-2841665.75	106.3880157	102218.1094	-6788.857422	0	0.5079653263

EELV.out

```
- Basic Output File -

Component           Iter          Shell Wt(lbs)       Frame Wt(lbs)       Total Wt(lbs)
interstage          0             1922.47436523       179.598571777        2102.0715332
lox_tank            0             2969.68237305       1016.21014404       3985.89160156
centerbody          0             2059.40454102       279.652984619       2339.05688477
lh2_tank            0             6857.89306641       2895.53320312       9753.41796875

                      Total vehicle shell weight:                     16907.2226562 lbs
                      Total vehicle frame weight:                     4258.69775391 lbs
                      Total vehicle structural weight:                21165.9277344 lbs
-----------------------------------------------------------------------------------------------

Component           Iter          Shell Wt(lbs)       Frame Wt(lbs)       Total Wt(lbs)
interstage          1             1913.75610352       178.787567139       2092.54394531
lox_tank            1             2957.48706055       1020.31835938       3977.80688477
centerbody          1             2047.73303223       280.781555176       2328.51464844
lh2_tank            1             6815.00195312       2894.82519531       9709.82617188

                      Total vehicle shell weight:                      16830.453125 lbs
                      Total vehicle frame weight:                     4261.78466797 lbs
                      Total vehicle structural weight:                21092.2324219 lbs
-----------------------------------------------------------------------------------------------

Component           Iter          Shell Wt(lbs)       Frame Wt(lbs)       Total Wt(lbs)
interstage          2             1913.69995117       178.782012939       2092.48046875
lox_tank            2             2957.35351562       1020.36309814       3977.71557617
centerbody          2             2047.63037109       280.793212891       2328.42333984
lh2_tank            2             6814.54931641       2894.81542969       9709.36914062

                      Total vehicle shell weight:                     16829.6679688 lbs
                      Total vehicle frame weight:                     4261.81982422 lbs
                      Total vehicle structural weight:                21091.4882812 lbs
-----------------------------------------------------------------------------------------------

Component           Iter          Shell Wt(lbs)       Frame Wt(lbs)       Total Wt(lbs)
interstage          3             1913.69946289       178.781967163       2092.47998047
lox_tank            3             2957.35180664       1020.36401367       3977.71435547
centerbody          3             2047.62902832       280.793334961         2328.421875
lh2_tank            3             6814.54980469       2894.81567383       9709.37109375

                      Total vehicle shell weight:                     16829.6621094 lbs
                      Total vehicle frame weight:                     4261.82080078 lbs
                      Total vehicle structural weight:                21091.4824219 lbs
-----------------------------------------------------------------------------------------------
Component           Iter          Shell Wt(lbs)       Frame Wt(lbs)       Total Wt(lbs)
interstage          4             1913.69946289       178.781967163       2092.47998047
lox_tank            4             2957.35180664       1020.36401367       3977.71435547
centerbody          4             2047.62902832       280.793334961         2328.421875
lh2_tank            4             6814.54980469       2894.81567383       9709.37109375

                      Total vehicle shell weight:                     16829.6621094 lbs
                      Total vehicle frame weight:                     4261.82080078 lbs
                      Total vehicle structural weight:                21091.4824219 lbs
-----------------------------------------------------------------------------------------------

Component           Iter          Shell Wt(lbs)       Frame Wt(lbs)       Total Wt(lbs)
interstage          4             1913.69946289       178.781967163       2092.47998047
lox_tank            4             2957.35180664       1020.36401367       3977.71435547
centerbody          4             2047.62902832       280.793334961         2328.421875
lh2_tank            4             6814.54980469       2894.81567383       9709.37109375

                      Total vehicle shell weight:                     16829.6621094 lbs
                      Total vehicle frame weight:                     4261.82080078 lbs
                      Total vehicle structural weight:                21091.4824219 lbs
-----------------------------------------------------------------------------------------------
```

EELV.siz

Structure Sizing File for EELV (with LRBs)

Shell and Frame Thicknesses, Semi-major and -minor axes, Density, and Maximum Running Loads vs. Fuselage Length

X(in)	Shell(in)	Frame(in)	a(in)	b(in)	rho(lb/in^3)	Nx_max(lb/in)	Ny_max(lb/in)	Nxy_max(lb/in)
0	2.58556	1.95765e-08	1	1	0.065029	99382.9	0	99373.9
1	1.42676	1.3618e-07	1.85	1.85	0.065029	58079.4	0	53713.3
2	0.985271	4.36862e-07	2.7	2.7	0.065029	40902.8	0	36802
3	0.752445	1.00875e-06	3.55	3.55	0.065029	31549.1	0	27989.1
4	0.608622	1.93903e-06	4.4	4.4	0.065029	25672.8	0	22581.2
5	0.510956	3.31493e-06	5.25	5.25	0.065029	21640.4	0	18924.4
6	0.4403	5.22372e-06	6.1	6.1	0.065029	18702.3	0	16286.7
7	0.38681	7.75275e-06	6.95	6.95	0.065029	16466.5	0	14294.2
8	0.344907	1.09894e-05	7.8	7.8	0.065029	14708.1	0	12735.9
9	0.311196	1.50211e-05	8.65	8.65	0.065029	13289.1	0	11483.9
10	0.283486	1.99353e-05	9.5	9.5	0.065029	12119.9	0	10456
11	0.260308	2.58196e-05	10.35	10.35	0.065029	11139.8	0	9596.87
12	0.240633	3.27616e-05	11.2	11.2	0.065029	10306.4	0	8868.16
13	0.223723	4.08489e-05	12.05	12.05	0.065029	9589.13	0	8242.26
14	0.209033	5.01691e-05	12.9	12.9	0.065029	8965.22	0	7698.84
15	0.196153	6.081e-05	13.75	13.75	0.065029	8417.59	0	7222.6
16	0.184768	7.28595e-05	14.6	14.6	0.065029	7933.06	0	6801.82
17	0.174631	8.64053e-05	15.45	15.45	0.065029	7501.31	0	6427.34
18	0.165549	0.000101535	16.3	16.3	0.065029	7114.17	0	6091.91
19	0.161625	0.000109225	17.15	17.15	0.065029	6765.06	0	5789.73
20	0.161625	0.000109328	18	18	0.065029	6448.64	0	5516.1
......								
......								
2280	0.250989	0.0151519	100	100	0.101	13435.4	0	1830.39
2281	0.251326	0.0151335	100	100	0.101	13454.3	0	1830.68
2282	0.251663	0.0151152	100	100	0.101	13473.3	0	1830.98
2283	0.252001	0.0150969	100	100	0.101	13492.2	0	1831.28
2284	0.252338	0.0150787	100	100	0.101	13511.2	0	1831.57
2285	0.248496	0.0159978	100	100	0.101	13600.2	0	780.782

EELV.sum

```
Delta-IV Heavy (with LRBs)
overall length 2285
Vehicle Geometry (position,semi-major,semi-minor axes):
0       1       1
20      18      18
198     100     100
2285    100     100

Vehicle Weight (description,start,end,weight):
fairing                        0       462              7860
interstage                   463       942        2092.47998
lox_tank                     943      1218       3977.714355
strap_ons                   1328      1328            114602
centerbody                  1157      1387       2328.421875
lh2_tank                    1388      2196       9709.371094
thrust_str                  2197      2285             10492
main_engine                 2285      2285             15394
aft_skirt                   1734      1822              3488
tunnel_assem                 942       942              1439
assem_prod1                  363      2285               680
prop_prod                    463      2285              2010
assem_prod2                    0      2285               279
2nd_stage                    463       942             68662
payload                      180       462             54282
propellant                   943      1218            377143
propellant                  1388      2196             62857
propellant                  1327      1328            754286
propellant                  1327      1328            125715

Structural Components:
lox_tank
lh2_tank
centerbody
interstage

Default Shell Configuration: z-stiffened
Default Material: aluminum
Material Definition (material,start,end,shell configuration)
aluminum                     943      1218      sandwich
aluminum                    1388      2196      sandwich
composite                    463       942      z-stiffened
composite                   1219      1361      z-stiffened
composite                      0       462      sandwich

Loadcase Definitions:
Loadcase #1
title:            Liftoff
x1:             2284
x2:             2285
axial_accel:        1.1945
normal_accel:     6.92e-05
prop_ullage:      30      30      30      30
pct_fueled:       100     100     100     100
Loadcase #2
title:            Max q
```

```
x1:                0
x2:             2285
axial_accel:          1.44
normal_accel:       0.0001
prop_ullage:            30      30      30      30
pct_fueled:       71      71      67      67
Loadcase #3
title:            Max q-alpha
x1:                0
x2:             2285
axial_accel:         2.193
normal_accel:        0.514
prop_ullage:            30      30      30      30
pct_fueled:     53.3    53.3      36      36
Loadcase #4
title:            Max Thrust
x1:                0
x2:             2285
axial_accel:        5.6162
normal_accel:       0.0012
prop_ullage:            10      10      10      10
pct_fueled:     7.28    7.28      10      10

Total number of iterations:         4
Total number of weights defined:    19
Total number of load cases:         4
Total number of materials defined:  5
-------------------------------------------------------------------
Total vehicle shell weight:         16829.6621 lbs
Total vehicle frame weight:         4261.8208  lbs
Total vehicle structural weight:    21091.4824 lbs
```

<u>Appendix G: Load Variation for each Load Condition of EELV Verification Case</u>

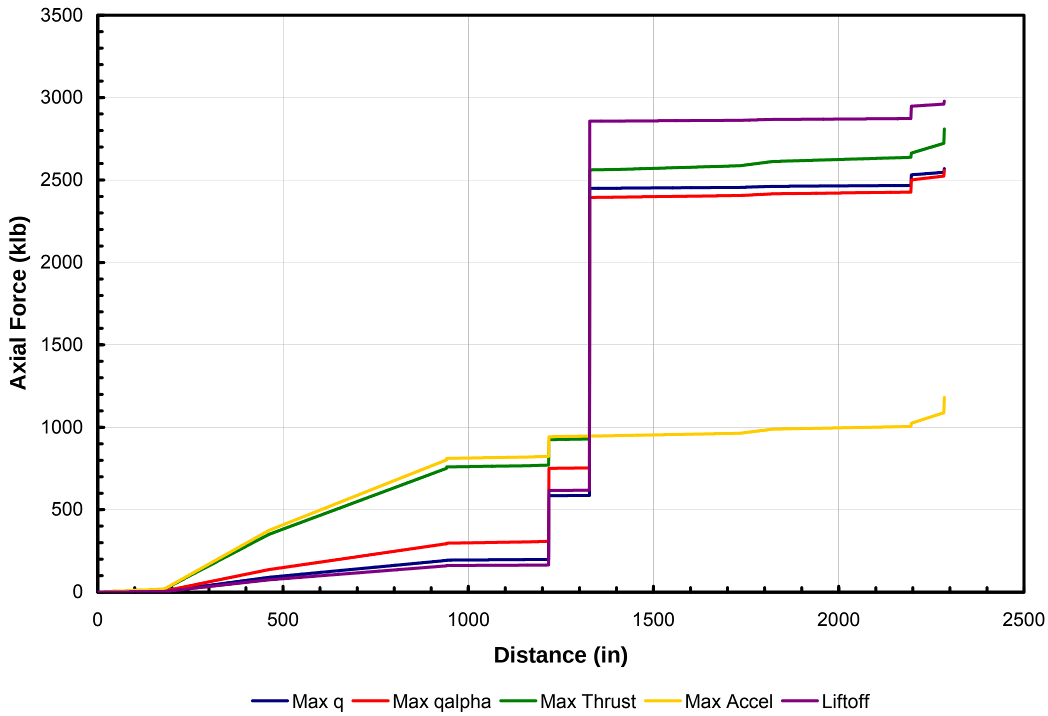

Figure 27. Axial Force Magnitude Variation along the Fuselage for each Load Condition of the EELV

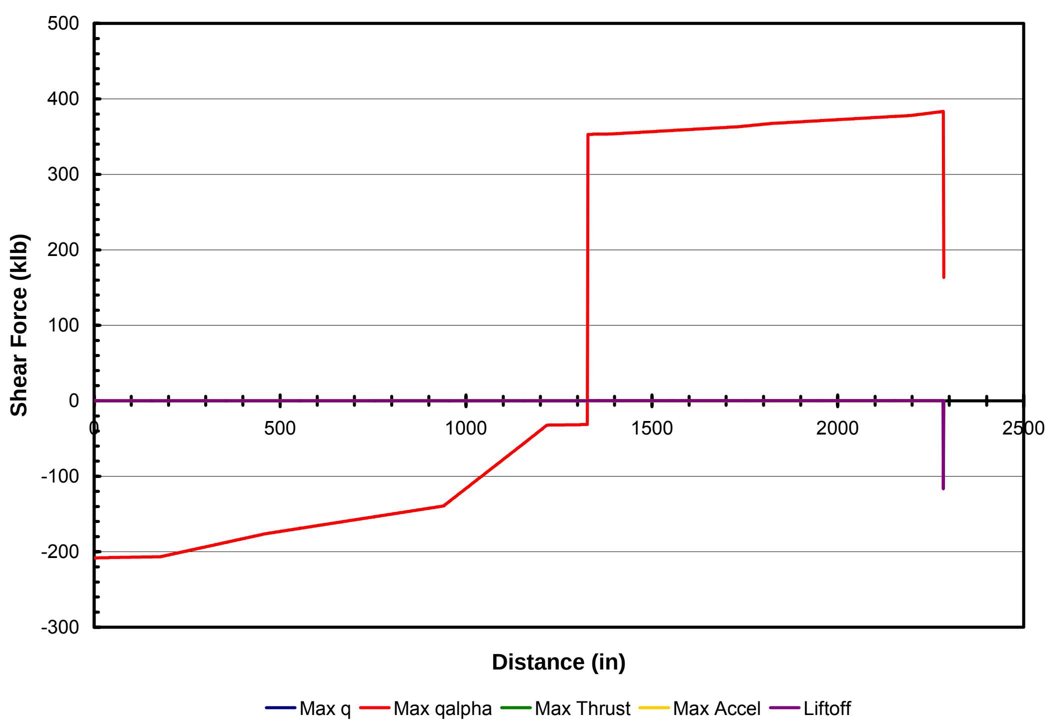

Figure 28. Shear Force Variation along the Fuselage for each Load Condition of the EELV

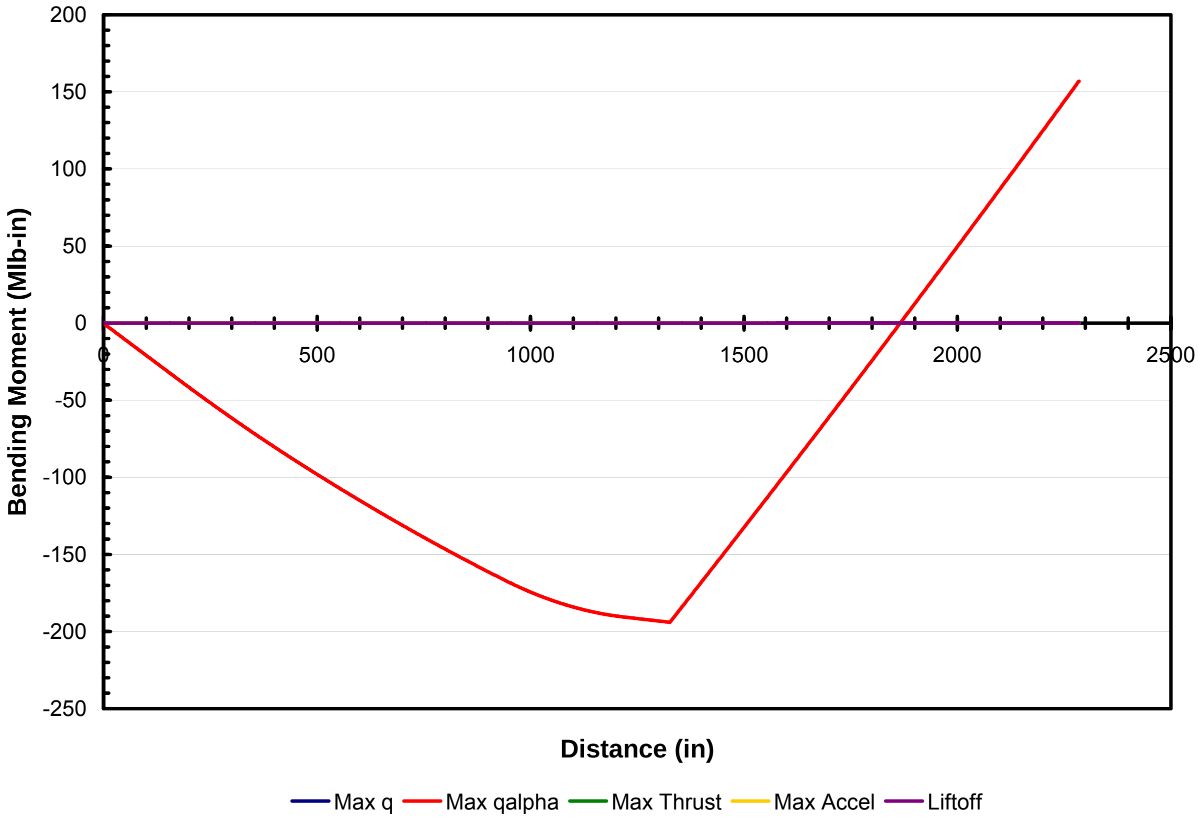

Figure 29. Bending Moment Variation along the Fuselage for each Load Condition of the EELV

Appendix H: Load Variation for each Load Condition of ET Verification Case

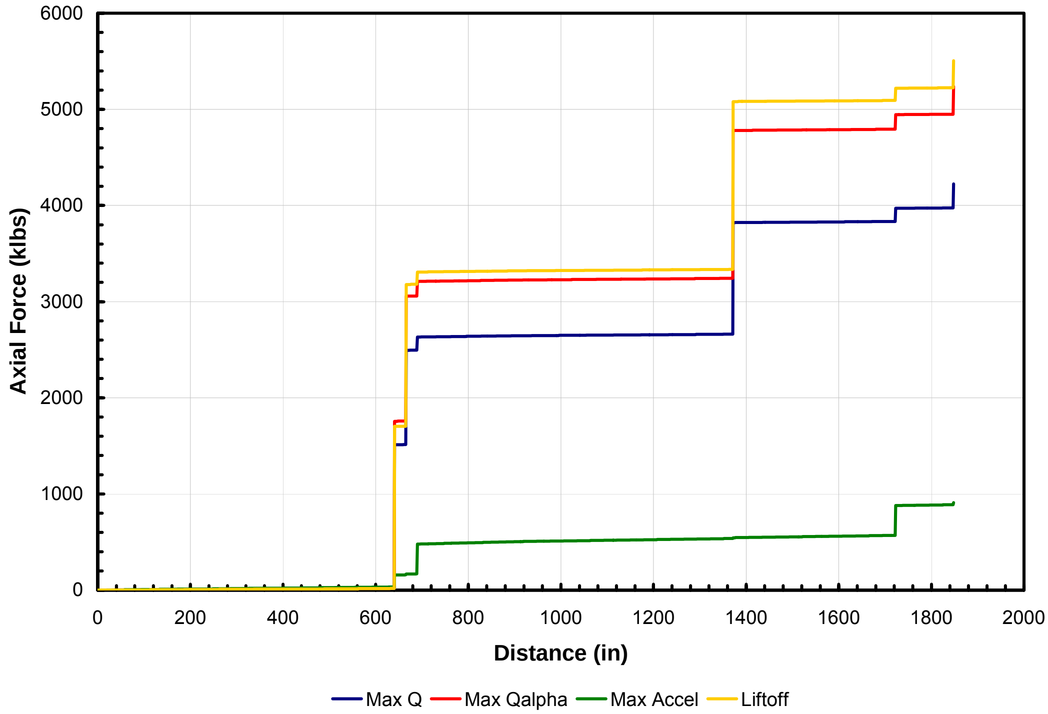

Figure 30. Axial Force Magnitude Variation along the Fuselage for each Load Condition of the ET

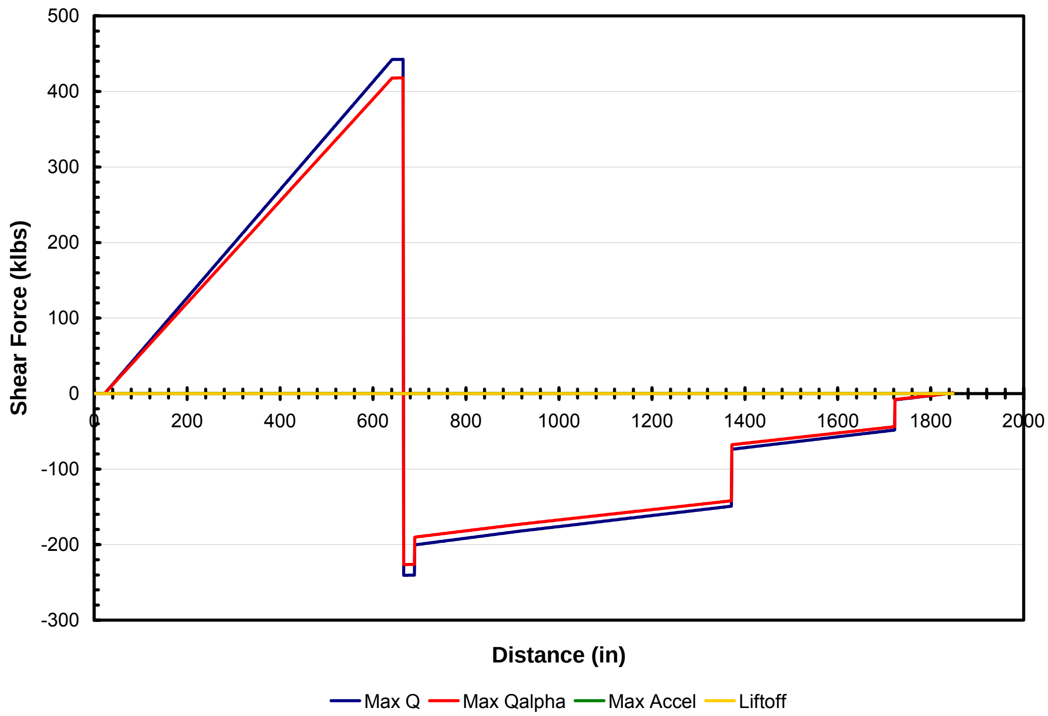

Figure 31. Shear Force Variation along the Fuselage for each Load Condition of the ET

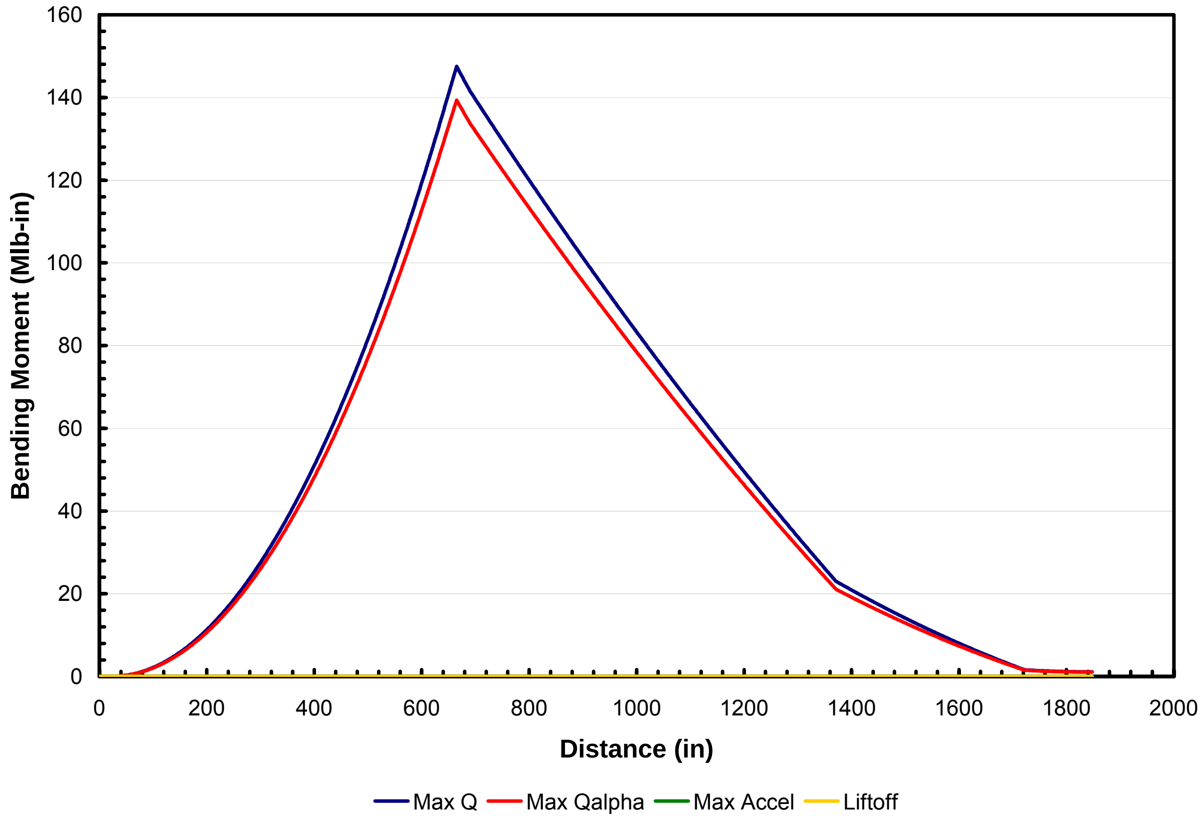

Figure 32. Bending Moment Variation along the Fuselage for each Load Condition of the ET

Appendix I: Contributing Analyses Spreadsheets used within ModelCenter

Trajectory CA: EELVPOST.xls

Condition	Time (s)	Axial accel. (axb), ft/s^2	Normal accel. (azb), ft/s^2	Propellant Used (wprus1), lb	Propellant Weight (440000 lb - wprus1), lb	LH2 Propellant Weight, lb	LOX Propellant Weight, lb	Axial Accel., G's	Normal Accel., G's	% LH2	% LOX
Liftoff	0	38.4253	0	0	440000	62857.14286	377142.8571	1.194445	6.92E-05	100.00%	100.00%
Max Dynamic Pressure	90	52.7263	-18.1268	159643	280357	40051	240306	1.44	0.0001	71.00%	71.00%
Max Q-Alpha	100	57.1586	-16.5409	177381	262619	37517	225102	2.193	0.514	53.00%	53.00%
Max Thrust	230	180.673	-0.03794	407976	32024	4574.857143	27449.14286	5.616195	-0.001179	7.28%	7.28%
Max Axial Acceleration	235	193.044	-0.0206	416844	23156	3308	19848	6.000746	-0.00064	5.26%	5.26%
MECO (same as Max Axial Accel.)											

Weights and Sizing CA: EELVWBS.xls

Generic Weights & Sizing Spreadsheet

First Stage	Level 2	Level 1		Output from STRESS	Correlated Weight
1 Structure		**45563.86**	Centerbody	3719	7056.0587
1.1 Primary Structure	**17235.07**		Interstage	5365	10179.0145
1.2 Fuel Tank	**14945.41**		LOX Tank	4926	6731.379
1.3 Oxidizer Tank	**6731.379**		LH2 Tank	10937	14945.4105
1.4 Thrust Structure	2010				
1.5 Sec. Structure	4642				

Legend

From ModelCenter

Correlated Weights

Constant

Calculated Weight